Indian Geotech J (February 2019) 49(1):2–36
https://doi.org/10.1007/s40098-019-00351-z

ARTICLE OF PROFESSIONAL INTEREST

Novel Techniques to Simulate and Monitor Contaminant–Geomaterial Interactions

Devendra Narain Singh[1]

Published online: 1 March 2019

Abstract Generation of huge amount of the toxic and hazardous wastes coming out of various industrial and domestic activities is becoming a major threat to the society. In the long run, mainly because of nonscientific storage, disposal and closure, and due to the presence of undesirable concentration(s) of chemicals and radionuclides, elevated temperatures and microbial activity, these wastes (read *contaminants*) interact with geomaterials, viz., soils, rock mass, groundwater. This interaction, termed as *contaminant-geomaterial* interaction, depending upon the severity of the contaminant(s) and interaction time, might alter overall characteristics of the geomaterials. Unfortunately, conventional laboratory and field instrumentation techniques are not well equipped to capture such interaction(s) and the mechanisms that prevail in the geomaterials. Hence, to achieve these objectives, evolving adequate and workable strategies, and modalities, that are nondestructive, noninvasive and economical is desirable. In this context, author's association with several industries resulted in development of innovative, cost-effective, yet efficient *techniques* that facilitate laboratory and/or in situ simulation and monitoring of such interaction(s). Details of these techniques, the philosophy behind their creation and the way they can be employed for safeguarding geoenvironment, from deterioration, are presented and discussed in this paper. Also, a brief discussion on some of the real-life situations where such techniques can be applied easily, by suitably modifying them, is presented for the benefit of the aspiring researchers and professionals.

✉ Devendra Narain Singh
dns@civil.iitb.ac.in

[1] Department of Civil Engineering, Indian Institute of Technology Bombay, Mumbai 400076, India

Keywords Geoenvironment · Toxic and hazardous waste · Waste disposal · Contaminant · Geomaterial · Interaction · Instrumentation · Monitoring · Simulation

Introduction

Various industries, considered as the backbone of a nation and responsible for making it *powerful* and *self-reliant,* viz., manufacturing, pharmaceutical, oil and gas exploration, thermal power plants, atomic power generation, research and medication installations, dredging and mining, generate huge amount of hazardous and/or toxic waste [56, 136, 144, 152, 153, 173]. Furthermore, activities like agriculture, construction and demolition, and 'domestic discharges' are responsible for generation tremendous amount of the municipal solid waste, MSW. Keeping in view the *sustainable growth*, ideally, strategies to utilize such waste, as a *man-made resource*, should have been practiced. In this context, it is heartening to note that these issues are being recognized by the researchers, planners, industries and the administration as a *major threat* for the society [40, 63, 64, 90, 91, 168, 169], and *ready-to-adopt techniques* that have potential to overcome this situation are being developed, marketed and implemented.

However, in order to safeguard the ecosystem against the wrath of such a situation, the waste, which might inherently contain leachable heavy metals and radionuclides, designated as *contaminants*, should be isolated from the *geoenvironment* by proper containment, encapsulation, immobilization, vitrification and/or disposal in deep geological formations [58]. An easy way to visualize the *geoenvironment* is to think of the subsurface domain, the *geomicrobiological sphere,* that mainly comprises the soil

and rock mass, microorganisms and groundwater [126–129, 138]. In the long run, these *contaminants*, due to their *interaction* with the rain water and/or fluctuating groundwater table, which act as a nemesis for the units (read canisters in case of the radionuclides) in which the waste is contained, tend to contaminate the *geoenvironment*.

Incidentally, attributes like chemical activity, high temperatures and the presence of radionuclides, in contaminants, and inherent characteristics of the geomaterials, viz., mineralogy and the presence of organic matter, pose a great challenge in evolving a proper and workable strategy to deter geoenvironmental degradation. To add to this list of woes, which makes this situation more *complex*, but *realistic*, the microbial (bacterial, fungal, pathogenic, viral and algal) activities pose a major threat to the geoenvironment. Incidentally, the author, a *geotechnical engineer* who as a student was averse to *biology*, was induced to take up this challenge by *biosavvy* and *enthusiastic* young researchers [106, 164–167, 190]. Another challenge being faced, in this context, is the *multi-phase* state of geomaterials, which makes it *not-so-easy* task to *simulate* and *monitor* the influence of *contaminants* on *geomaterials* and the mechanisms prevailing in them [26, 72, 73]. From this discussion, it can be realized that handling, storage and disposal of toxic and hazardous wastes, and identifying/establishing their impact on the geoenvironment (by conducting environmental impact assessment, EIA) are becoming an utmost priority [4, 48–50, 54, 137, 141].

For safe execution of geotechnical engineering projects, various laboratory and field *instrumentation techniques* and *testing protocols* that facilitate characterization of geomaterials have already been developed. And this knowledge has also been adopted and prescribed by various statutory agencies such as FHWA (Federal Highway Administration, USA), ASTM (American Society for Testing and Materials) International, USA, BS (British Standards), EC (Eurocode), BIS (Bureau of Indian Standards) and EPA (Environmental Protection Agency), in the form of *codal provisions*. These protocols are quite useful to capture *macro-characteristics* of geomaterials, viz., strength, compressibility and hydraulic conductivity, which are mainly driven by *mechanical stresses* (better designated as *stimuli*), only. However, for a situation like *contaminant-geomaterial* interaction, picturized above, capturing *micromechanisms,* viz., diffusion, dispersion, sorption and desorption, decay/decomposition, deposition, erosion and suffusion, exo- and endothermic reactions, heat and moisture migration, cracking, rheology and coupling of these mechanisms, becomes very crucial [43]. Needless to state, these mechanisms are driven by *environmental factors,* viz., humidity, temperature, solar cycle, wind speed and rainfall intensity, and might evolve due to chemical, thermal, electromagnetic, radiation and microbial activities. These factors can be designated as *environmental stimuli,* and their influence on overall characteristics (physical, chemical, mineralogical and biological) of the geomaterials and the mechanisms that prevail in them, should be investigated rigorously when *contaminant-geomaterial* interaction occurs [74–77]. Needless to emphasize, all this falls beyond the realm of the *conventional geotechnical* methodologies and techniques and hence resorting to an interdisciplinary approach becomes inevitable.

Furthermore, the situation becomes dire when reputed and established equipment manufacturers shy away in extending their helping hand to the research fraternity, due to several reasons and constraints, viz., lack of interest, inertia to adopt and practice new concepts, fear of not fulfilling supply–demand chain, lack of financial viability. However, this turned out to be *a blessing in disguise* and prompted the author and his research group (designated as *THE ENVGEO*s) to deal with simulation and monitoring *contaminant-geomaterial* interaction. This incidentally was the starting point of our journey in the realm of geoenvironmental engineering [181]. A brief account of the research and development contributions made by *THE ENVGEO*s, in context of simulating and monitoring short- and long-term *contaminant-geomaterial* interaction and *the prevailing mechanisms*, is presented in the following. In due course of time, these techniques, which are a trend-setter, indigenous, economical and ingenious, became a panacea for solving various geoenvironmental issues highlighting the fact that *there is nothing called a problem, it's just absence of an idea to find, the solution*.

Types of Contaminant–Geomaterial Interaction

Based on the above discussion, it becomes imperative that efforts should be made to simulate, and quantify, *contaminant-geomaterial* interaction, which would be very useful for addressing various *geoenvironmental issues* that the contemporary society is facing, in a precise manner. The changes undergone by the geomaterials, when contaminants (exhibiting attributes like elevated temperatures, chemical and radionuclide concentrations) interact with them. This would be quite important and crucial for designing structures such as liners of waste containment facilities, landfills, cores of the dam, which are primarily constructed from fine-grained soils, treatment and stabilization of highly contaminated soils and dredged sediments, stabilization of soft and sensitive soils and construction of roads and airfields by resorting to thermal treatment [169, 228].

The possible situations when *contaminant-geomaterial* interaction are: (1) passive geomaterial interacting with water, which corresponds to minimal interaction, viz., sands–water interaction, (2) active geomaterial interacting with water, viz., fine-grained soil–water interaction, which could result in heat of wetting, *HOW*, (3) passive geomaterial interacting with contaminants, viz., sands–contaminant interaction, and (4) active geomaterial interacting with contaminants, viz., fine-grained soil–contaminant interaction. These interactions might occur in *geoenvironment* due to either *natural or man-made activities*. Hence, the effect of these activities on overall properties of the geomaterials (pre- and post-interaction) should be investigated [191, 193, 195]. In this context, though, researchers have employed various *techniques* and *instrumentation,* viz., batch tests, column tests, lysimetric studies, geotechnical centrifuge modeling and impedance spectroscopy, to monitor and quantify *contaminant-geomaterial interaction*, under controlled environmental conditions, most of these studies are contaminant and geomaterial specific and hence cannot be generalized, especially when *soils* are exposed to higher concentrations and temperatures associated with the contaminants.

Quantification by Using k_d Parameter

The *contaminant-geomaterial* can be quantified by employing a parameter, designated as *distribution coefficient*, k_d. It has been demonstrated by Arnepalli et al. [4], Pathak et al. [127, 128] that several parameters, viz., specific surface area, *SSA*, cation-exchange capacity, *CEC*, percentage organic matter, percentage of fines, *CL*, mineralogy, redox potential, type of ionic species and their concentration, *pH*, temperature, liquid to solid ratio, *L/S*, and interaction time, influence determination of k_d, which requires very intricate experimental investigations. Hence, design of the *batch tests* to minimize the experimental efforts, and to understand the influence of so many parameters on k_d, becomes most desirable. Also, due to interplay of these parameters, it becomes difficult to identify the parameter(s) which would have the most significant influence on k_d. It should be noted that identification of such parameter(s) would be helpful in optimizing the number of tests to be conducted for determining k_d of a *contaminant-soil system*, CSS, which otherwise is a very cumbersome task. To achieve this, *Taguchi method*, which primarily helps in designing experiments [206], was employed for the (i) identification of the most significant parameters on which k_d depends and (ii) *estimating* k_d by inputting these parameters, in the form of a *lookup table*, which would be quite handy for all those who design and analyze different types of CSSs, as described in the following.

Various soils such as white clay (designated as WC), bentonite (designated as BT), five natural soils, namely S1, S2, S3, SS1 and SS2, collected from different parts of India, were used. Further, $SrCl_2$, $CaCl_2$, $CdCl_2$, $HgCl_2$, $ZnCl_2$, $FeCl_3$, $NiCl_2$, and nitrates of thorium, uranium, lead and cobalt in their nonradioactive form, were employed as the model contaminants. Batch tests were conducted following the guidelines presented in the literature [4, 7], and various *sorption/desorption isotherms* were employed to compute the respective k_d [127, 128]. The effect of concentration of contaminants on k_d was standardized by employing *electrical conductivity*, σ, of the some of the *contaminant-soil solutions* during sorption and desorption processes, as depicted in Fig. 1. The data depicted by solid and open symbols, in the figure, correspond to sorption and desorption processes, respectively, for various CSSs.

It can be observed from Fig. 1 that, as expected, σ increases with an increase in initial concentration, C_i, of the contaminants used in the study. This highlights the fact that the contaminant contributes more in the value of σ of the CSS as compared to the soil.

However, the reverse phenomenon takes over when σ of the CSS increases due to leaching of the cations present in the soil, when it interacts with the lower concentration of the contaminant. These facts can be elaborated further by employing a term *critical concentration* or *critical molarity*, M_{crt}, depicted as a vertical dotted line in Fig. 1. Incidentally, this line demarcates contribution of soils toward *desorption* (marked as a left side arrow, when soil is dominating in the CSS) and *sorption* mechanisms (marked as a right side arrow, when contaminant is dominating in the CSS). Hence, it can be opined that the concentration of the contaminant plays a very crucial and decisive role in determination of k_d of the CSS. As such, establishment of M_{crt}, by conducting batch tests with a wide range of concentration of contaminants and determining the sorption mechanism prevailing in a certain concentration range of contaminant, becomes mandatory to obtain meaningful k_d. To establish the influence of C_i on k_d, three cases of the σ versus C_i relationship (refer Fig. 2), which also exhibit the M_{crt}, were considered. These cases are: (i) C_{FULL}, (ii) $C_{Mcrt\text{-}Min}$ and (iii) $C_{Max\text{-}Mcrt}$, as depicted in Fig. 2, where C_{FULL}, $C_{Mcrt\text{-}Min}$ and $C_{Max\text{-}Mcrt}$ exhibit concentration ranges from 0.5 to 1×10^{-7} M, M_{crt} to 1×10^{-7} M and 0.5 M to M_{crt}, respectively.

Furthermore, *kinetic and thermodynamic* studies for various CSSs were conducted on soils BT, WC, S1, S2, S3 and contaminants $SrCl_2$, $Pb(NO_3)_2$ and $UO_2(NO_3)_2$, which are the major isotopes present in radioactive waste, by performing batch tests. The kinetic reaction depends upon the interaction between the sorbate–sorbent (i.e., the contaminant-soil) system [8], which also helps in determining the changes in the concentration of the sorbate over a

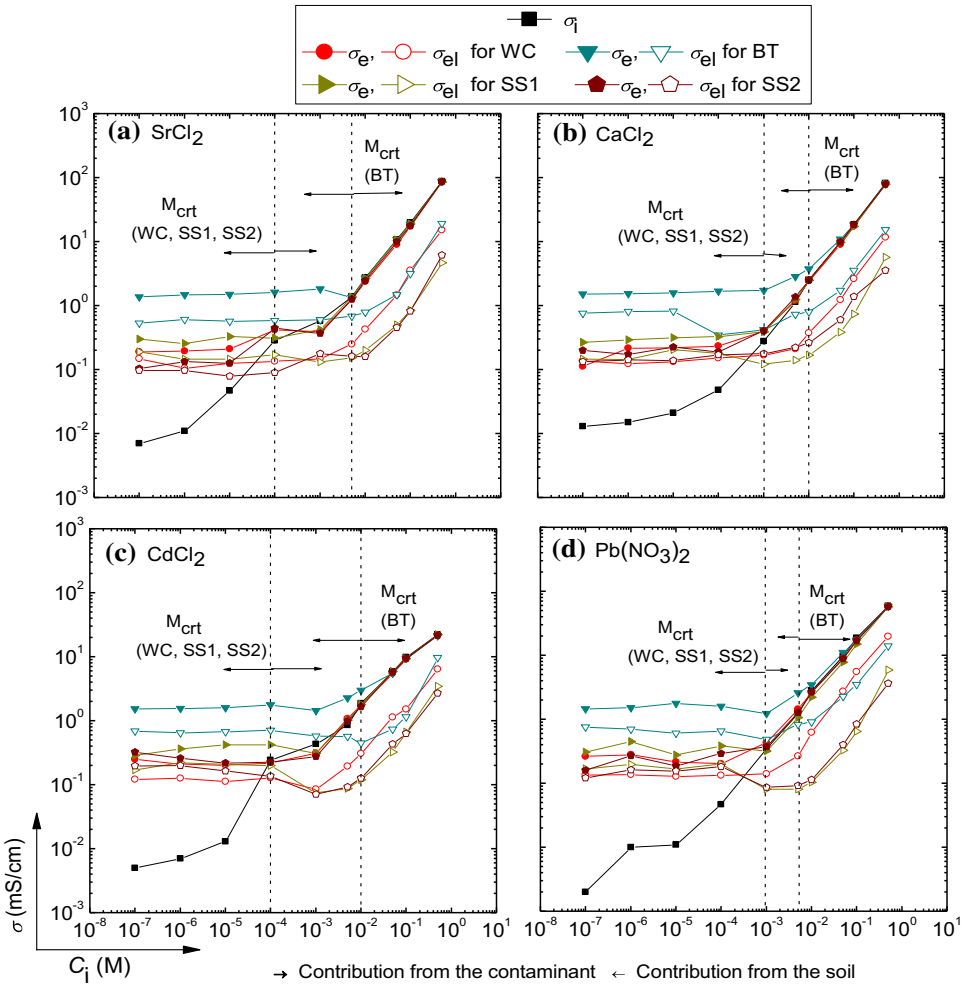

Fig. 1 Variation of electrical conductivity after sorption and desorption for different CSSs

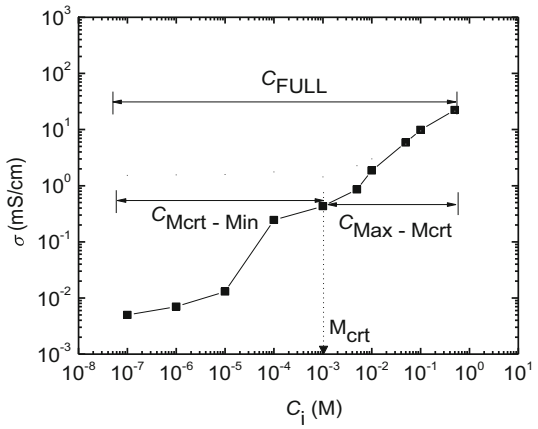

Fig. 2 The three cases of the initial concentrations of the contaminant considered for determination of the k_d

certain duration. As such, the sorption rate of the contaminants onto the soil particles (i.e., the sorption mechanism) was also studied. As temperature is an important factor that influences the sorption characteristics of the soil [220], batch tests were performed by varying temperature, T (viz., 27 ± 2 °C, 35 ± 2 °C and 45 ± 2 °C), while the interaction time of CSS, *L/S,* soil *pH*, soil and contaminant species was maintained unchanged. The thermodynamic studies were performed to understand (i) how energy changes and/or dissipates in the CSS and (ii) the nature of reaction (i.e., spontaneous or nonspontaneous) within this system.

As mentioned earlier, *Taguchi method* was used to design batch tests by employing L25 orthogonal array, *OA*, referred by Taguchi and Konishi [206] and Wu and Zhou [224], which is a special matrix having optimal setting of maximum six parameters and minimum two parameters with five setting levels (i.e., the experimental conditions). It is based on the selection of the five parameters in the study (refer Table 1).

However, it should be realized that for investigating the influence of these five parameters on k_d, 5^5 (= **3125**) experiments need to be conducted, *which turns out to be a mammoth task*. This necessitates establishment of sensitivity of the k_d on the various attributes of the soil-contaminant system, as discussed above. Such a sensitivity

Table 1 Selection of the input parameters and experimental conditions

S. N.	*L/S*	C_i (M)	Contaminant	*CEC* (meq/100 g)	pH_i
1	10	0.1	$SrCl_2$	105.05	1
2	20	0.02	$CaCl_2$	82.41	3
3	50	0.003	$CdCl_2$	77.39	5
4	100	0.0005	$Pb(NO_3)_2$	54.58	6
5	200	0.0001	$HgCl_2$	37.59	7

analysis would be helpful in minimizing the number of experiments, otherwise required, to determine k_d. Moreover, for investigating the influence of these parameters on k_d, a wide range of experimental conditions were chosen for quantifying the *contaminant–soil* interaction. Subsequently, batch tests were designed for five different parameters and five experimental conditions, as mentioned in Table 1. Accordingly, L25 *OA* was found suitable, and only 25 batch tests were performed for understanding the mutual influence of the five parameters. Based on this analysis, a *lookup table* (refer Table 2) for various CSSs was also developed. The *lookup table* is a quick interface for estimating k_d for different types of *contaminant-soil systems* and can be utilized for proper design and execution of various geoenvironmental projects mentioned earlier.

The efficiency of the *lookup table* should be verified for several *contaminant-soil systems* by conducting batch tests. The methodologies based on *electrical* and *microwave* impedances should be developed for determination of k_d, a panacea for detecting the influence of the waste on the geoenvironment.

Quantification by Using XRD, Nanoindentation and LSD Techniques

Kadali et al. [74] attempted to: (a) develop a methodology, which can be employed for quantifying *contaminant–soil interaction*, under laboratory conditions, and (b) investigate the changes undergone by the soil, when it interacts with the contaminants (possessing both high temperature and concentration). To achieve this, the state-of-the-art *instrumentation* and *techniques,* viz., laser scanning diffraction, X-ray diffraction stress analysis and nanoindentation, have been employed. Such a study has been found to be very handy to develop a *soil characterization scheme*, based on the parameters that imbibe physical, chemical and mineralogical characteristics of the soil, and can easily and quickly be determined in any conventional geotechnical engineering laboratory, as described in the following.

The mechanical and engineering characteristics (such as hardness, residual modulus and resistance to indentation) of the geomaterial were determined up to 200 °C, in steps of 50 °C, by employing a nanoindenter (Model: TI 900 Tribolndenter, marketed by Hysitron, USA). This

Table 2 The "lookup table"

Soil	pH	Soil characteristics							Contaminant characteristics				Output
		CL	*SSA*	CEC_T	RWL	Minerals	MO	ξ	Cationic species	pH	*T*	T_e	
BT	7.5	90	621	105	33.80	M	4.27	33.50	U, Th	3	27	6	k_d (l/kg)
WC		54	49	38	48.63	K	3.62	17.50	Pb, Cd	4	35	12	
S1	6.2	31	23	82	56.55	Ma, Mu	10.60	14.50	Ca, Sr	5	45	24	
S2	5.2	70	21	64	70.18	Mu, Bi	1.60	24.89	Co, Zn	6	55	36	
						Ml			Fe, Ni	7	65	48	
S3	7.1	44	289	61	83.48	Mu	2.94	12.50	Hg	8		72	
SS1	7.3	0	629	77	42.73	Q, He	4.55	19.21					
						Ma							
SS2	7.8	0	279	55	29.78	Q, C	7.66	27.51					

CL clay fraction (in %), *SSA* specific surface area (in m^2/g), CEC_T total cation-exchange capacity (in meq./100 g), ξ zeta potential (in -mV), *RWL* reactivity with lime (in %), *MO* summation of CaO, K_2O and Na_2O (in %), *T* temperature (in °C), T_e interaction time (in hr.), *M* montmorillonite, *K* kaolinite, *Ma* magnetite, *Mu* muscovite, *Bi* biotite, *Ml* mullite, *Q* quartz, *He* hematite, *C* calcite

equipment contains a CCD camera, attached to an optical microscope (refer Fig. 3a). A Berkovich indenter (refer Fig. 3b) which is a three-sided pyramid of *radius of curvature* ~ 150 nm and measures the force imposed on the pellet (read specimen, refer Fig. 3c), was employed for these investigations. The corresponding displacements are recorded with the help of LVDTs.

The investigations conducted by Kadali et al. [74] have revealed that the *changes* in the color of soils, heated up to 250 °C, can be attributed to depletion of the organic matter, primarily [117, 216]. However, corresponding to the temperatures greater than 250 °C, except for the soils containing kaolinite, this phenomenon could be attributed to an increased oxidation and other *chemico-mineralogical* changes [76]. An increase in the *specific gravity* and decrease in the *specific surface area*, *SSA*, of the soil, due to its exposure to elevated temperatures, has also been observed. This phenomenon can be attributed to the loss of moisture, the presence of the organic matter, impurities and changes occurring at elemental level. It has also been observed that, except for the soils with passive minerals, viz., quartz and kaolinite, the clay-sized fraction decreases, while the silt-sized fraction increases with an increase in temperature. This observation further substantiates that exposure of the soil to elevated temperatures results in an increase in its particle size. The decrease in the *SSA* of the soil can further be substantiated by an increase in its particle size due to its exposure to elevated temperatures, as substantiated by *laser scanning diffraction* analysis. Interestingly, it has been observed that the cation-exchange capacity, *CEC*, of the soil decreases as the exposure temperature increases. This can be attributed to a reduction in the exchangeable cations and loss of organic matter present in the soil [22, 172]. Furthermore, a reduction in zeta potential [3, 80, 107, 218, 222, 226] of the soil, which defines its capacity to interact with the environment (read water, air, gases, contaminants), due to its exposure to elevated temperatures and excess contaminant concentrations, has also been observed [2, 21, 55, 81, 103, 225]. The investigations by employing X-ray diffraction were instrumental in demonstrating, successfully, that with an increase in exposure temperature, θ, the lattice spacing changes (refer Fig. 4), which indicates mineralogical *phase transformation*.

Here it is worth reiterating that the changes in crystallographic characteristics of the geomaterial would strongly influence its physical and chemical properties. It has also been observed that with an increase in temperature, the soils containing passive minerals, viz., quartz and kaolinite, exhibit *expansion*. On the contrary, soils containing active minerals, viz., montmorillonite, *shrink*, due to the loss of *hygroscopic moisture* [134, 157]. Furthermore, the investigations conducted by Kadali et al. [75] were instrumental in demonstrating the utility of X-ray diffraction analysis for establishing *residual normal* and *shear stresses* on the soil grains when they get exposed to the elevated temperatures [199, 204, 205, 221]. These researchers were also successful in demonstrating the potential of *nanoindentation*, which is mostly employed by material scientists for characterization of metals, in identifying the changes undergone by the fine- and coarse-grained soils when they get exposed to elevated temperatures [27, 132]. A typical load versus displacement response of a soil exposed to different temperatures is depicted in Fig. 5.

Based on our studies, we could also demonstrate that the fine-grained soils, in contrast to the coarse-grained soils, are more susceptible to changes in *hardness*, *H*, *residual modulus*, E_r, and *resistance to indentation*, h_{max}, when exposed to elevated temperatures (refer Fig. 6). However, efforts should be made to extend these studies by considering (a) the interaction of different types of contaminants and geomaterials of entirely different species, exposed to elevated temperatures, (b) quantification of such interaction and derivation of generalized relationships and (c) investigations related to the alteration in various geotechnical properties of the soils (viz., shear strength, compressibility, compaction characteristics, permeability) due to such interaction(s).

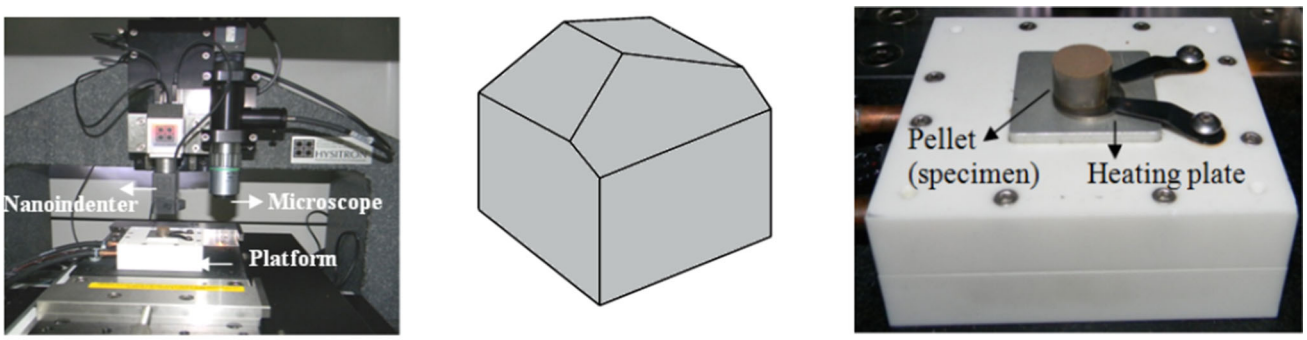

Fig. 3 The setup depicting **a** nanoindenter along with the microscope, **b** the Berkovich indenter and **c** the specimen mounted on the heating plate

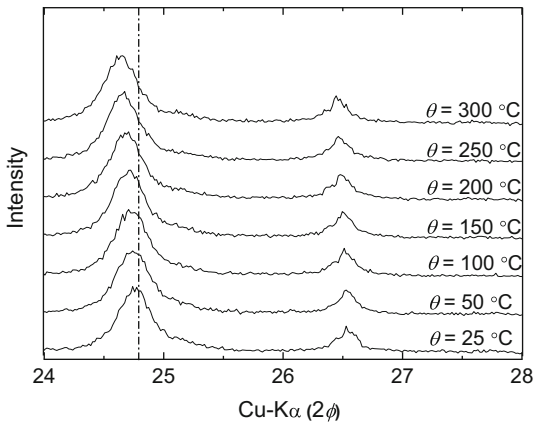

Fig. 4 The X-ray diffraction patterns of the soil exposed to different temperatures

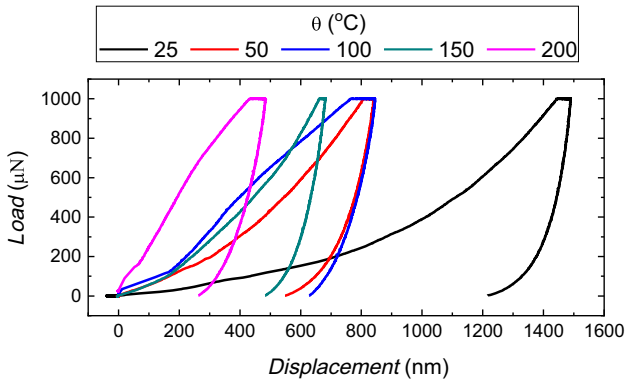

Fig. 5 Typical load vs. displacement response, obtained from the nanoindentation, for the soil exposed to elevated temperatures

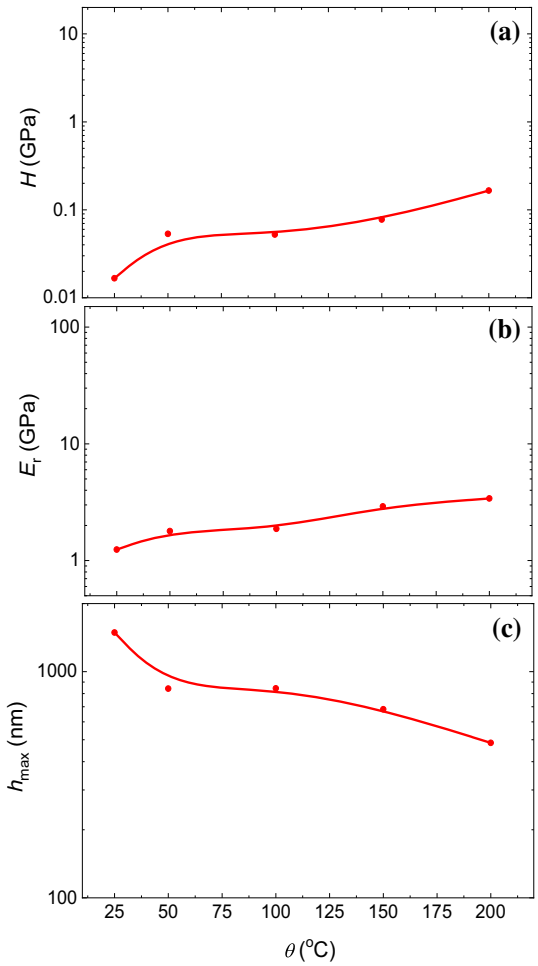

Fig. 6 Variation of the **a** hardness, **b** residual modulus and **c** maximum depth of indentation with respect to temperature for a typical soil

Quantification by Using Heat of Wetting

As mentioned earlier, the heat of wetting, *HOW*, is an interesting philosophy to quantify *contaminant (in fluid phase)* and *geomaterial* interaction. In case of the fluid that is a *liquid*, the setup employed for quantifying the *HOW* would be similar to the one used by professionals that work on *cementitious materials and admixtures,* i.e., a calorimeter or a heat of hydration setup. However, when the liquid gets replaced with the *gas*, more intricate setups that would facilitate its *adsorption and/*or *sorption* on the geomaterials (this process is a precursor to *sequestration*) need to be created or employed [136].

The *HOW* setup, to simulate *contaminant-geomaterial* interaction when the latter is in liquid form, consists of a calorimeter, which is a wide-mouth vacuum flask of 500 ml capacity, fitted at the top with a cork stopper containing two holes. Through one of these holes, a funnel for pouring the sample in the flask is fitted, while the second hole facilitates fitting of a T-type thermocouple, which records temperature of the solution, when connected to a datalogger. The calibration of the thermocouple was carried out by inserting it in boiling water and ice. A stirrer, which is rotated by a motor at a constant speed, has been provided to facilitate proper mixing of the *soil* and *contaminant* in the liquid form. This simple setup has been found to be quite useful for quantifying *contaminant-geomaterial* interaction, as explained in the following.

As depicted in Fig. 7, the temperature, θ, versus time, t, trends for the soils of entirely different chemical constituents, could be utilized for computing the *HOW* of a geomaterial in its contaminated or uncontaminated states.

As depicted in Fig. 7, the θ versus t trends for the soils can be grouped into three categories: **A, B** and **C**, mainly depending upon their characteristics. While both trends **A** and **B** exhibit a sharp increase in θ, in case of the former, temperature attains almost a constant value, θ_c, with time, while in case of the latter, it drops down sharply from a peak temperature, θ_p, followed by attainment of the constant temperature value, θ_c. In author's opinion, these

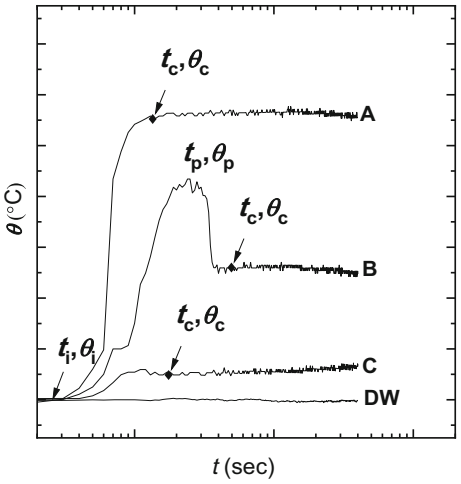

Fig. 7 The variation of temperature with time for *HOW* tests

trends, in general, exhibit *soil–water interaction*, which primarily depends upon the physical, chemical and mineralogical characteristics of the soil [15]. However, trend **C** indicates very less interaction, as the changes in values of θ are almost negligible. Subsequently, the percentage increase in the temperature of the soil–water mixture, *PIT* [= $(\theta_c - \theta_i) \bullet 100/\theta i$], can be computed. It should be noted that θ_i corresponds to the ambient temperature, for $t = 0$ s. Another parameter, the reaction time, *RT* (= $t_c - t_i$), has been defined, which quantifies the minimum time required by the *soil–water* slurry to attain the constant temperature, θ_c. It is author's hunch that *RT* is related to the *PIT* and hence it should be a measure of the potential of the soil to release heat (due to exothermic reaction) when it comes in contact with water. This study demonstrates the utility of the parameter, *HOW*, which has been quantified as the percent change in temperature of the fine-grained soils when they are allowed to interact with water (or for that matter any contaminant in the solution form) in a calorimeter. However, as during this interaction, the physical, chemical and mineralogical properties of soils play an important role, this parameter has been related to various soil-specific properties, viz., clay fraction present in the soil, *CL*, plasticity index, *PI*, liquid limit, *LL*, specific surface area, *SSA*, and cation-exchange capacity, *CEC*. Based on extensive investigations, on fifty soils of entirely different characteristics, it has been demonstrated that there exists a well-defined relationship between these parameters and the *PIT*, refer Fig. 8 [77].

It is believed that the relationships proposed in Fig. 8 can be employed for determining the soil-specific parameters, particularly the fine-grained soils, just by determining the *PIT*, which can be obtained easily, and quickly, by employing a calorimeter. Needless to mention, this philosophy (read technique) will be a boon for the researchers and professionals dealing with the characterization of soils. However, it is recommended that extensive studies should be conducted, by the research fraternity, to check the validity and utility of the proposed relationships (Fig. 8) and to refine them if they are found misleading. A big leap in this context would be to evolve a *novel soil classification system* for characterizing the soils by utilizing the parameter *PIT*, which includes in it the physical, chemical and mineralogical characteristics in a holistic manner.

Gas–Geomaterial Interaction

Some good examples of *gas–geomaterial interaction* are: remediation of contaminated soils by air sparging [145], carbon sequestration [154], radioactive waste disposal [104] and gas permeation in porous media [151]. Incidentally, determination of specific surface area, *SSA*, of geomaterials, by employing: (a) Blaine's air permeability apparatus [6] and (b) absorption/adsorption techniques, wherein methylene blue, nitrogen gas, ethylene glycol monoethyl ether, EGME and air, are employed [5], is another good examples of *gas–geomaterial* interaction.

Another challenging but industry-relevant problems that Shanthakumar et al. [159, 160] studied is *flue gas conditioning*, FGC, of the fly ash, as described in the following. It is a well-understood fact that among various pollution control devices, electrostatic precipitators, ESPs, and cyclone separators, are popularly employed by the thermal power stations, and cement plants, for reduction of suspended particulate matter, SPM, as depicted in Fig. 9a. This is mainly due to their greater efficiency in removing particles (< 0.01 μm in size), their effectiveness in a wide range of operating temperatures and their suitability for corrosive environmental conditions. However, the constraints associated with *implementing* various measures to enhance performance of ESPs at a power station are: (i) constraints associated with the feed coal (i.e., cost associated with import, washing of the coal and environmental issues associated with it and ash content), (ii) addition of more collection plate area in the ESP [34], which requires more space and is highly expensive, (iii) the installation and operating costs for employing wet ESPs are too high apart from lump formation of the ash, and its degradation as a construction material [178]. Under these circumstances, the FGC becomes the inevitable choice, mainly due to the fact that the (i) lower cost input compared to the establishment of additional ESPs, (ii) shorter execution time, (iii) more flexibility and versatility even if variations in operating parameters occur (such as coal variation, boiler load, ESP voltage and current change); SPM levels can be controlled/maintained easily by simply adjusting the amount of FGC agents. These agents are quite

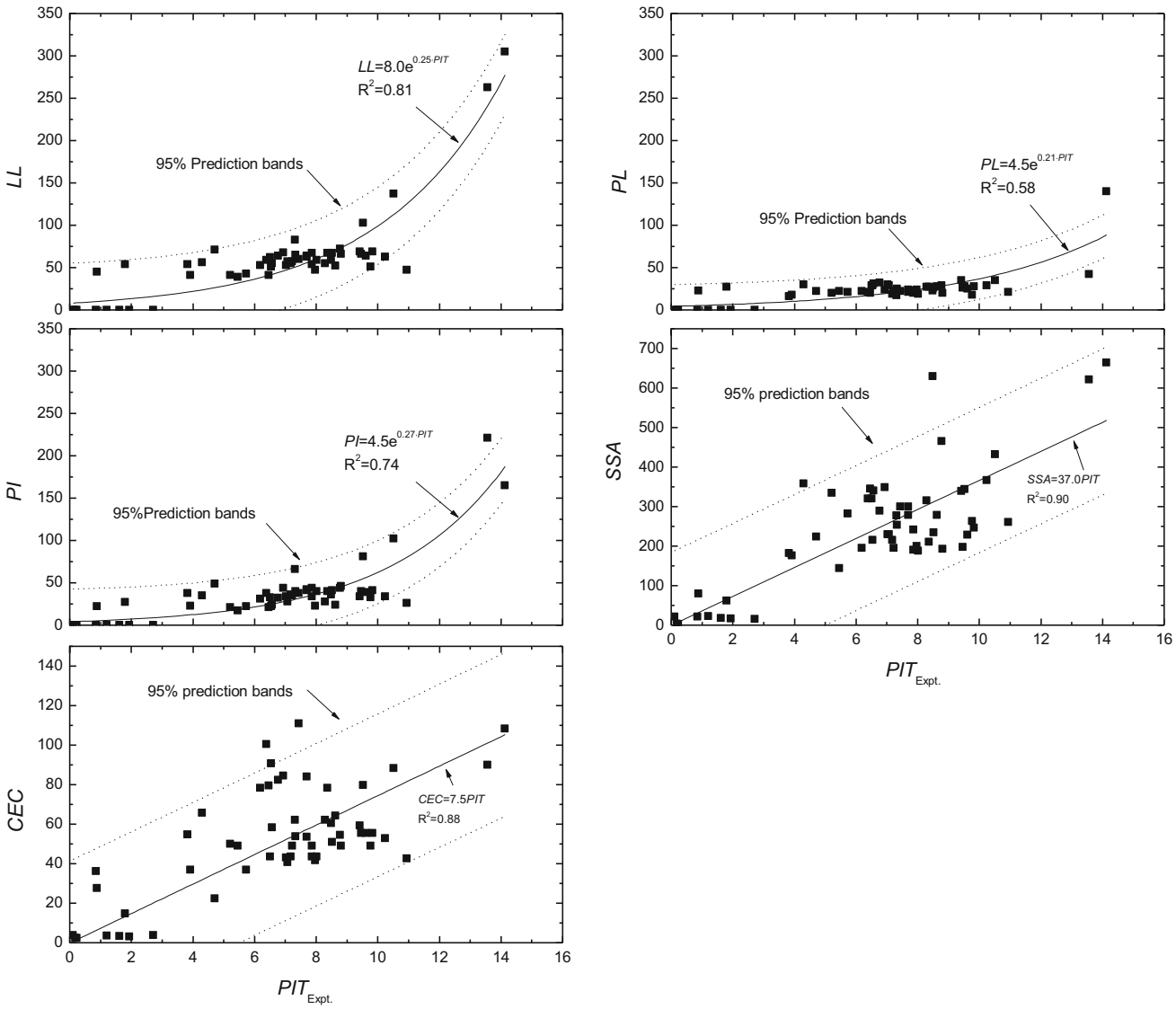

Fig. 8 The variation of *LL*, *PL*, *PI*, *SSA* and *CEC* with the *PIT* obtained from *HOW* experiments

useful in reducing resistivity, R, refer Fig. 9b, and hence improving the surface conduction characteristics of the particles of fly ash/dust [162].

Apart from this, researchers have demonstrated and critically evaluated the importance of the FGC by resorting to different techniques, viz., sulfur trioxide conditioning, ammonia conditioning and dual flue gas conditioning, DFGC [161]. It has been reported by these researchers that during conditioning of the flue gas, a part of the conditioning agent (particularly ammonia) gets *precipitated* on the fly ash particles, which might influence its overall characteristics and hence its *utility and marketability*. The conditioned ash might also lead to contamination of both the ground and surface water, if disposed in a landfill.

To answer these issues, comprehensive studies were conducted to investigate the influence of FGC on physical, chemical, mineralogical, morphological and pozzolanic characteristics of the fly ash. Also, how FGC results in improved performance of the ESPs, and hence in a reduction of the SPM emission levels, should be studied extensively keeping in view the intricate *gas–geomaterial interaction*, which is essential to design and model various environmental clean-up strategies.

In this context, the SEM micrographs of the fly ash (refer Fig. 10), after DFGC, reveal that this treatment is more effective for increasing the fly ash collection due to agglomeration of the ash particles, which enhances the collection efficiency of the ESP. This in turn results in less SPM emissions from the power plants levels [159–161, 163].

However, the growing emphasis on utilization of the fly ash, and cenospheres, has raised major concerns about the

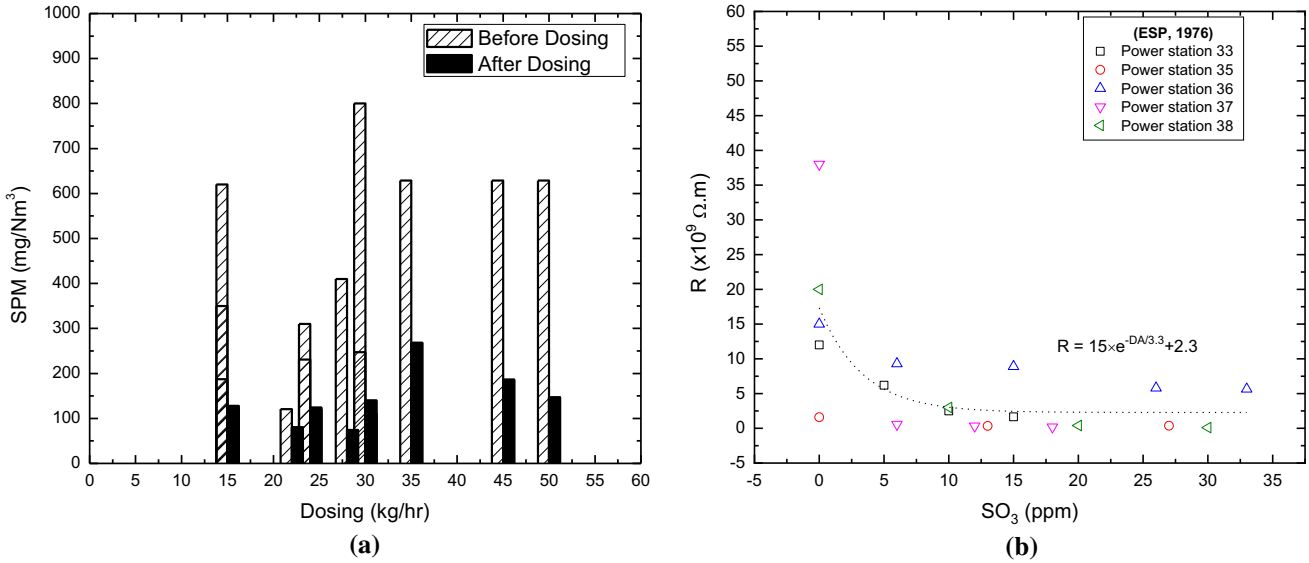

Fig. 9 **a** Efficiency of the FGC at various power stations in India. **b** The effect of SO_3 dosing on resistivity of the fly ash

Fig. 10 Micrographs of the fly ash after undergoing DFGC

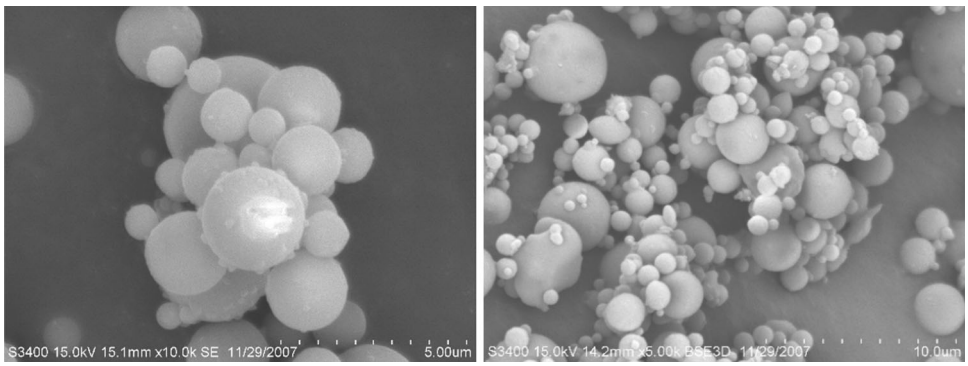

suitability of the conditioned fly ash in cement and concrete industry [10, 11, 29]. This is mainly due to the fact that the presence of residual conditioning agent might adversely affect the characteristics of the fly ash. Hence, it becomes essential to ascertain the extent of changes undergone by the fly ash in its physical, chemical, mineralogical, morphological and pozzolanic characteristics, as a result of the FGC. Also, the influence of FGC on the *collection efficiency* of the ESPs needs to be investigated, which would be of great help in developing a suitable strategy for controlling the SPM emission levels at thermal power stations.

In this context, studies conducted by Shanthakumar et al. [159–161, 163] turned out to be a big relief, for the power plants. These studies were instrumental in demonstrating that the *optimal dose* of the conditioning agent(s) does not alter the *lime reactivity* and *pozzolanic activity* [25] of the conditioned fly ash.

Effects of Contaminant–Geomaterial Interaction

When *contaminant-geomaterial interaction* occurs, depending upon the severity of this interaction, the geomaterial might undergo: (a) mineralogical alteration and (b) decomposition. These *micromechanisms* might result in *fabric* alteration of the geomaterial, as well, as explained in the following.

Mineralogical Alteration

One of the good examples of the *contaminant-geomaterial interaction* is 'alkali activation' of the fly ash, which results in mineralogical alteration of the fly ash [178]. Hence, apart from many applications of the fly ash, known to the construction industry [85–87, 183], its valorization in the form of 'fly ash zeolites,' FAZ, has gained significant attention of researchers in the recent past [65, 82, 83, 85].

The FAZs, viz., Na-P1, hydroxysodalite, faujasite, chabazite, analcime and cancrinite, are available in hydrated

alumino-silicate mineral forms and can be synthesized from the fly ash by its *adequate* alkali activation. However, the physical properties, viz., specific gravity, specific surface area, chemical composition, viz., silica and alumina contents, and mineralogy, viz., quartz and mullite, of the fly ash largely influence this process, the grades of FAZs formed, mostly quantified by the cation-exchange capacity, in particular [5, 16, 84]. Accordingly, the use of fly ash zeolites in industries, especially for removal of heavy metal ions and other wastes for various environmental clean-up projects, would primarily depend upon their *grade*, which would mainly depend upon the method adopted for the synthesis [86–90]. Over the years, several methods: (a) hydrothermal, (b) fusion prior to hydrothermal treatment, (c) microwave-assisted hydrothermal treatment and (d) molten salt technique have been adopted by researchers for achieving the desired *mineralogical alteration* of the fly ash (read synthesis of ash zeolites) [65, 66, 91, 92], as discussed in the following.

To simulate the effect of *contaminant-geomaterial* interaction on *mineralogical alteration* of the geomaterial, the mixture of the raw (or original) fly ash, RFA and different stock solutions of NaOH, was hydrothermally activated at 100 °C, in an open refluxed system, as depicted in Fig. 11. The activation duration was varied from 12 to 48 h, with an increment of 12 h [67–70]. After each step of interaction, the residues and the supernatant were processed and recycled, as depicted in Fig. 12a. The oven-dried residues from primary treatment, PT, were powdered, with the help of mortar and pestle, before each recycling step, R1 and R2. Both the residues and supernatant from each step were characterized, simultaneously. On the other hand, the three-step activation, TSA, by fusion of the fly ash, coated with NaOH (NaOH/RFA ratio varied from 0.2 to 1.4, at an increment of 0.2), was conducted at 500 °C for 2 h, in a muffle furnace [68]. To overcome the issues associated with inadequate contact between the RFA and NaOH, fused residues were powdered using mortar and pestle, before subjecting them to recycling steps of fusion, F2 and F3, as depicted in Fig. 12b.

The results obtained from these syntheses are presented in Figs. 13 and 14. Symbols Q, ML, P, C, S, F, H and M designate the quartz, mullite, zeolite Na-P1, cancrinite, hydroxysodalite, faujasite, hematite and molarity of the NaOH solution, respectively. The designations 1.5-PT, 1.5-R1 and 1.5-R2 correspond to the residues produced after steps 1, 2 and 3 of the TSA, respectively, by using 1.5 M NaOH and 12 h of activation in each step. The formation of polycrystalline phases of the FAZs can be observed in Fig. 13a, which can be attributed to a significant gain in the cation-exchange capacity, *CEC*, of the residues (up to 185%) after step 2 (refer Fig. 13b). Although step 3 causes less increase in the CEC, remarkable growth in the crystal shapes up to 830 nm (refer Fig. 14a) is indicative of enrichment with hydroxyl bonds and more –Si–O–Al-bonding (confirmed by a shift in the peak depicted in Fig. 14b). This indicates more crystallization in the residues, 1.5-R2 (refer Fig. 14b), as compared to the raw fly ash, RFA [33, 71].

However, efforts should be made to relate the cation-exchange capacity of the geomaterial with the silica/alumina ratio. Such a correlation would be very much useful for predicting the susceptibility of a geomaterial to get mineralogically altered. This philosophy would also be useful for the production of *synthetic minerals* at industrial scale for their application in various environmental clean-up projects.

Decomposition

The severity of the contaminants, in terms of elevated temperature, the concentration of the chemicals, radionuclides, microorganisms and environmental radiations, are primarily responsible for decomposition of geomaterials that consist of high organic matter, viz., humus, peats, marine clays, biochar, municipal solid waste. This process might result in generation of leachates, semisolids and

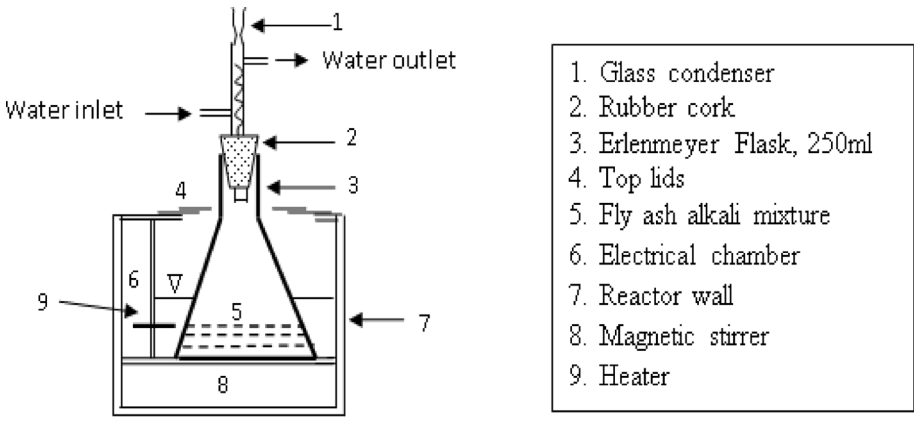

Fig. 11 Details of the reactor employed for hydrothermal activation of the fly ash

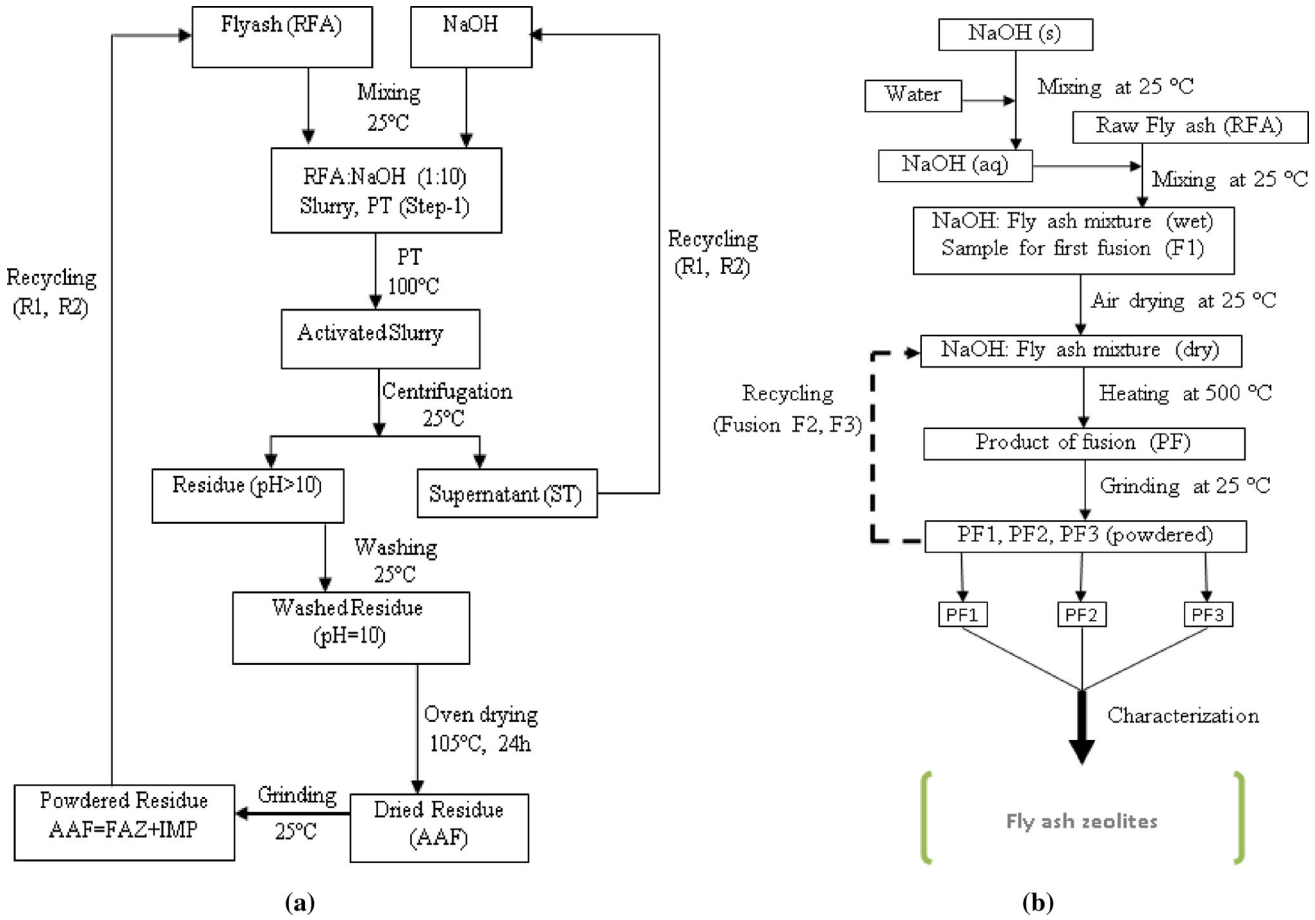

Fig. 12 The stepwise flow charts for the TSA of the fly ash by **a** hydrothermal and **b** fusion methods

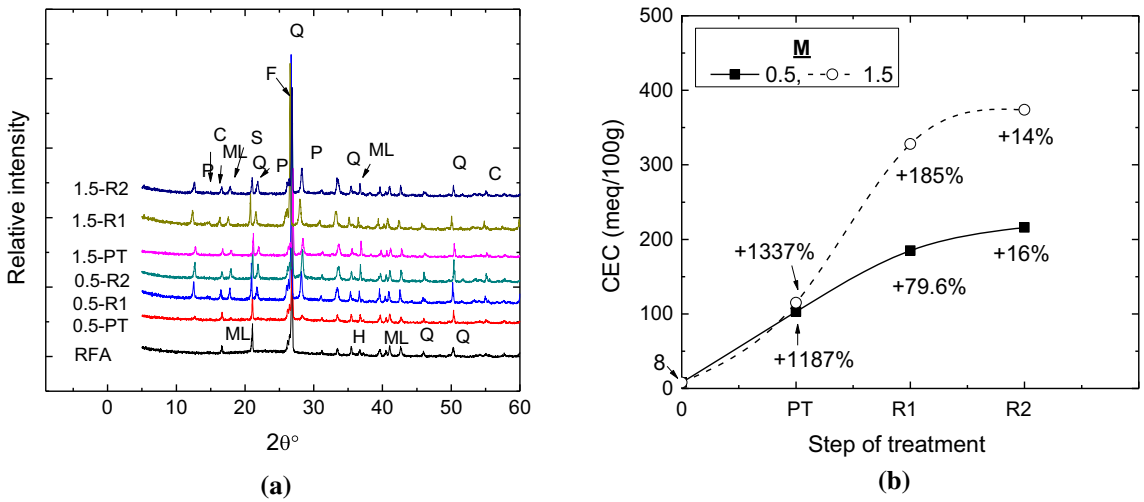

Fig. 13 The effect of the TSA on characteristics of the residues, changes in the **a** mineralogy and **b** CEC

gases, which tend to migrate through the appropriate *pathways* in the far- and near fields to contaminate the geoenvironment [137, 138]. The decomposed geomaterial should be treated as a 'multi-phase system,' and its conceptualization and modeling is the prime focus of *The ENVGEO*s, presently, as discussed in the following.

The major factors responsible for controlling the rate of decomposition of the municipal solid wastes, MSW, which author treats as the *manmade* resource, are the moisture

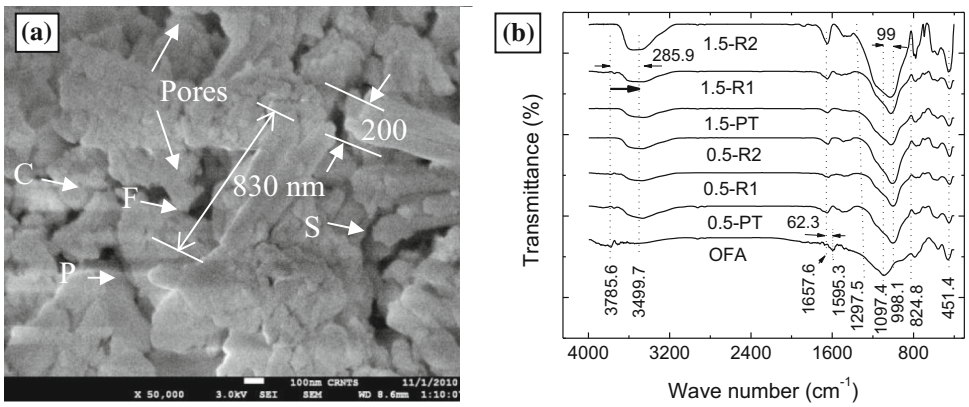

Fig. 14 The effect of the TSA on characteristics of the fly ash residues as confirmed from the **a** morphology of 1.5-R2-24 and **b** FTIR results

content, temperature and biological activities. To study the degradation characteristics of the MSW, sustainable engineered bioreactor landfill, SEBLF, was developed. As depicted in Fig. 15, a scaled-down field model of the SEBLF would facilitate: (a) demonstration of the effectiveness of the state-of-the-art *instrumentation,* viz., time and frequency domain reflectometry, TDR and FDR, probes and *multi-level* thermocouples, that is conceived for monitoring the moisture content and temperature, respectively, (b) to maintain the favorable conditions for bacterial activity, which would accelerate the decomposition rate by controlling the moisture content and temperature of the MSW inside the SEBLF, through scheduling of leachate recirculation, (c) to ascertain the controlled emission (and capturing) of biogas generated due to decomposition of MSW, (d) to analyze the leachate characteristics, which are indicative of the degree of decomposition, over a period of time, and (e) to assess groundwater and surrounding soil contamination [20, 130, 131].

To simulate decomposition of the MSW, under laboratory conditions, the (a) laboratory bioreactor landfill, designated as LBLF (ref. Fig. 16a), and (b) the SEBLF (ref. Fig. 16b), were developed. These setups have been found to be quite useful for conducting studies related to decomposition of the MSW.

The TDR and FDR probes and thermocouples were employed for monitoring and controlling the moisture content, W, and temperature, θ, at a certain depth in these reactors, respectively (refer Fig. 17). It should be noted that due to the spatial heterogeneity of the MSW, in its composition and density, the application of such probes and interpretation of the obtained results are a challenging task [201, 202]. Through this exercise, it has been realized that by proper scheduling of leachate recirculation [147], the rate of decomposition of the MSW can be augmented up to a great extent [130]. Furthermore, it has been demonstrated that due to the presence of various *macro- and micronutrients* in the *final harvested material* (the residues) of the anaerobic and aerobic BLFs could be an appropriate

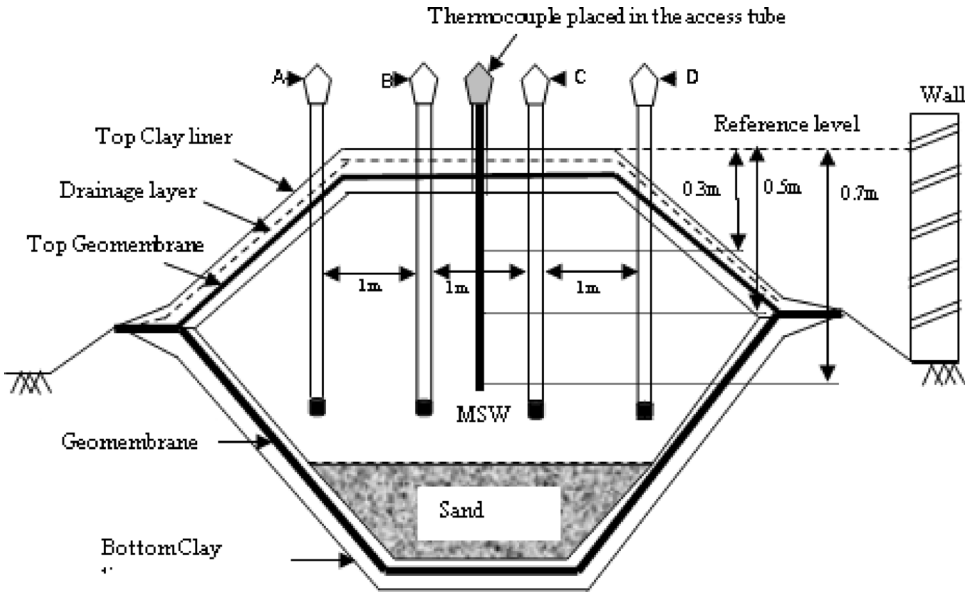

Fig. 15 Installation of the FDR probe and thermocouple in the SEBLF

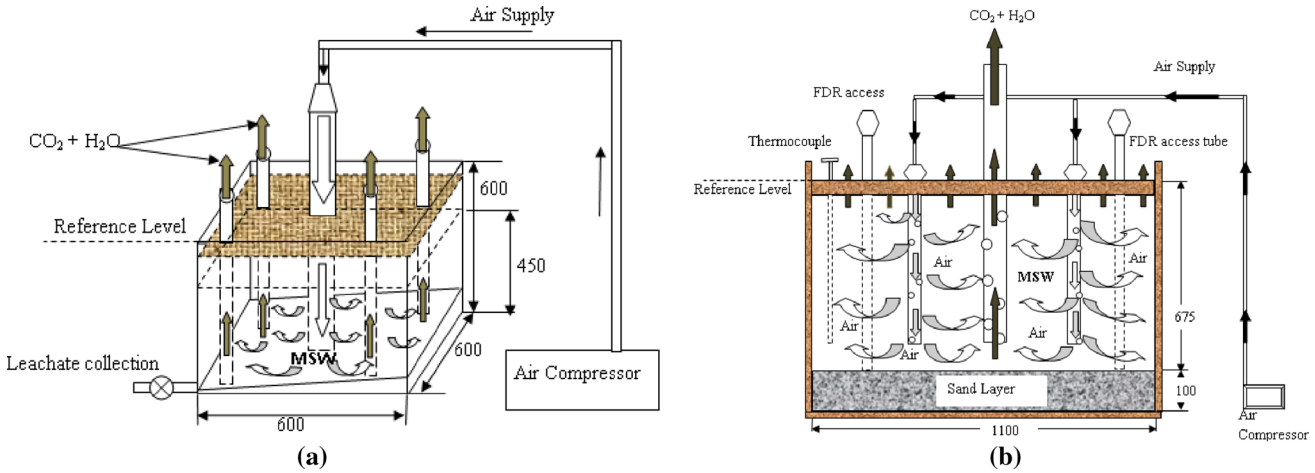

Fig. 16 **a** Schematic of the **a** laboratory bioreactor landfill, LBLF, and **b** sustainable engineered bioreactor landfill, SEBLF

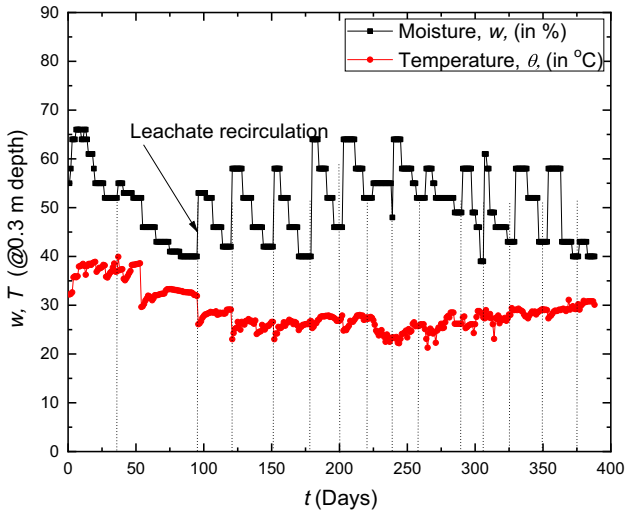

Fig. 17 Monitoring decomposition of the MSW by employing state-of-the-art instrumentation and leachate recirculation

replacement for the conventional manures and fertilizers [130, 146].

However, extensive studies are required, to study the effect of heterogeneity of MSW on the decomposition process in the bioreactor landfill. Development and application of the low-cost wireless sensors in the bioreactor landfills, which can be used for monitoring the pH, moisture content, temperature, constituents of the biogas and bacterial growth, appears to an idea worth trying. Also, *leachate augmentation* by treating it with microbes should also be tried.

Fabric Alteration

Based on the discussion presented above, it is easy to comprehend that when *contaminant-geomaterial* interaction occurs, the *fabric* of the geomaterial might get changed [35]. This is valid particularly for the particulate geomaterials, viz., soils mass, which consists of the particles and pores of various sizes and shapes, and their arrangement, nature and distribution are termed as *fabric*. These parameters, and hence the *fabric*, influence engineering properties of the soil mass, viz., shear strength, compressibility, rheology, conductivity of fluids, to a great extent [31, 44, 45]. Hence, quantification of the *fabric*, and its anisotropy, becomes important for a better understanding of their overall response to *external stimuli*, particularly in case of the fine-grained soils [32, 46]. In this context, a methodology based on electrical impedance measurement, termed as *impedance spectroscopy*, IS, for determining the *fabric* of the soil mass in its undisturbed, remolded, sedimented and *exposed to thermal flux* states was developed [17, 44, 45, 79, 150, 155–157, 198, 200]. Incidentally, this methodology has also been found to be extremely useful for quantifying the *fabric* anisotropy, as discussed in the following.

The undisturbed samples of the marine clays were collected from the eastern coast of India, with their depth ranging from 5 to 65 m, below the seabed. To obtain *fabric* characteristics of these samples, their electrical

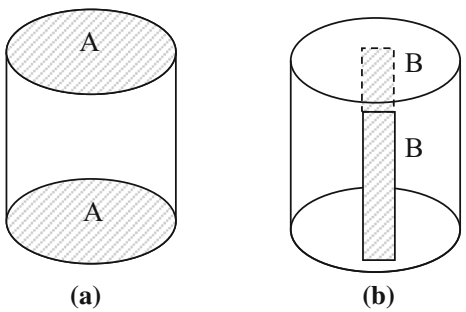

Fig. 18 Measurement of the impedance response of the sample on **a** longitudinal (A–A) and **b** transverse (B–B) planes

conductivity, σ, was measured across **A–A** (longitudinal direction) and **B–B** (transverse direction) as depicted in Fig. 18. The test setup depicted in Fig. 19 was developed and employed for this purpose [47].

Investigations to establish *fabric* of the sample were also conducted by resorting to scanning electron microscopy, SEM, and mercury intrusion porosimetry, MIP, on 5-mm cubical specimens, retrieved from the UDS or reconstituted samples, as depicted in Fig. 20.

These investigations reveal that *fabric* of the soil mass, and its anisotropy, could be quantified in terms of the electrical anisotropy, viz., the anisotropy coefficient, A_e. As such, in case of the soil mass exhibiting *flocculated fabric* (i.e., the random orientation of the particles) A_e will be equal to (or approaches) unity. On the contrary, in case of the soil mass exhibiting *dispersed fabric*, the A_e is much higher than unity (> 1.75). In case of the undisturbed marine clays, normally, A_e is very high (≈ 2) and it almost remains constant with the moisture content. However, in case of the samples retrieved from the same borehole, but from different depths, A_e is found to be strongly dependent on the sampling depth (the overburden). Incidentally, it is possible to classify or identify the type of *fabric* exhibited by the soil mass based on its A_e value, refer Fig. 21, which presents results obtained from the techniques like IS, SEM and MIP. Figure 21 is used as a guideline for determining the *fabric* (i.e., its type and corresponding mean pore diameter, d_m) of the fine-grained clays, if A_e is known. Incidentally, it should be appreciated that determination of A_e, by adopting the technique mentioned above, is quite easy, and less time-consuming, as compared to SEM and MIP techniques.

Hence, the advantage of IS over MIP and SEM, for determining *fabric* of the soil mass, in a nondestructive and noninvasive manner, and that too without facing the complexities associated with the sample preparation has been established. It must also be appreciated that the size of the sample and its moisture content are not a constraint for conducting the IS, as compared to its counterparts, and hence the results obtained would be more reliable.

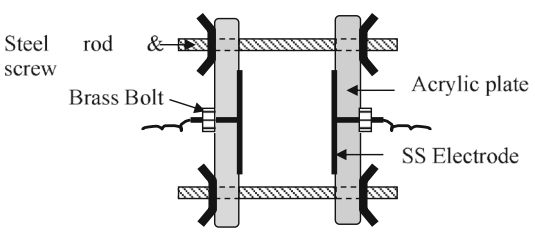

Fig. 19 The sample holder used for conducting impedance spectroscopy of the sample

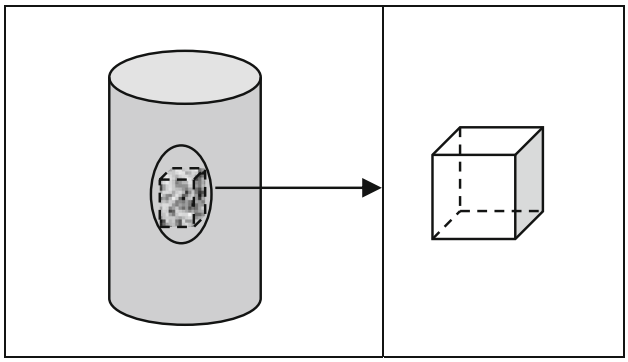

Fig. 20 Extrusion of the cubical specimen for establishing its *fabric*

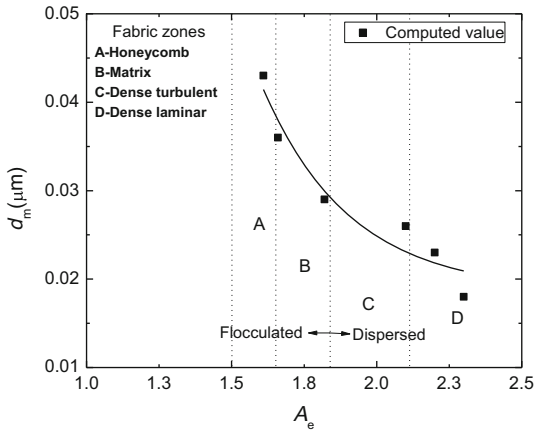

Fig. 21 Guidelines for determining *fabric* of the fine-grained soils

Alteration in Geomechanical Properties

It has been demonstrated by earlier researchers [100, 121, 122] that various geomechanical properties of the soil mass, viz., undrained shear strength, compression index, void ratio, elastic modulus and Poisson's ratio, can be determined in a noninvasive and nondestructive manner, easily, by correlating them to shear and compression wave velocities, V_s and V_p. Conventionally, resonant column, cyclic triaxial and torsional shear tests, which are quite intricate and expensive setups, have been employed for this purpose. However, *piezo-ceramics* (bender and extender elements) have been found to be very efficient in transmitting and receiving shear and compression waves [12, 14] without impacting the sample, as strains produced are $< 0.001\%$.

With this in view, a *piezo-ceramics* were developed from the lead zirconate titanate (LZT)-based material, which exhibits high dielectric constant [17], with high piezoelectric sensitivity, for low power consumption. Depending upon the requirements, these elements can be polarized in the same or opposite directions, as depicted in Fig. 22.

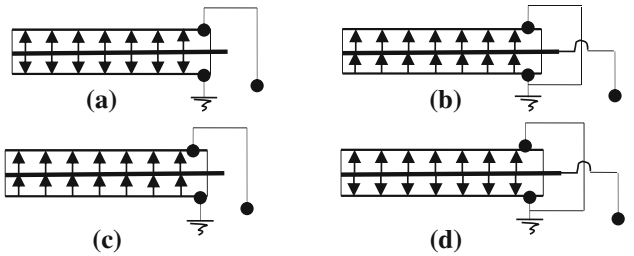

Fig. 22 Different configurations of piezo-ceramics: *benders* **a** opposite series and **b** same parallel and *extenders* **c** same series and **d** opposite parallel

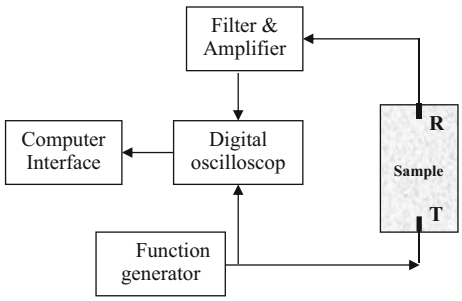

Fig. 23 The arrangement for transmitting and receiving waves in the sample

The block diagram depicted in Fig. 23 was developed for transmitting (T) and receiving (R) waves, and proper functioning of the piezo-ceramics was confirmed by hearing a 'sing' sound when excited with a sine-wave pulse from the function generator [14, 118, 120].

In order to check the versatility of these *piezo-ceramics*, V_s and V_p were measured on standard materials and also in asphaltic concrete and very soft clays [119]. V_s and V_p were also measured for different types of soils in their remolded and undisturbed samples, UDS, by employing the setups depicted in Fig. 24.

The above-mentioned discussion highlights that *piezo-ceramics* have already been utilized to characterize fine-grained and granular geomaterials. However, this technique should be employed to *detect* and *monitor* various micromechanisms, viz., *mineralogical alteration*, *decomposition* and *fabric alteration*, that prevail in the geomaterials (in their saturated, unsaturated, contaminated and multi-phase) when they interact with contaminants. In this direction, it would also be quite prudent if electrical properties (resistivity and dielectric dispersion) of the geomaterials could also be linked with the V_s and V_p.

Monitoring and Simulation of Contaminant Transport

The *contaminant-geomaterial* interaction would also result in transport of contaminants in the soil and rock matrix. However, this interaction would be guided by, primarily, (a) the type and condition of the rock mass (intact or fractured) and (b) the soil mass (saturated or unsaturated). The fractured rock mass and the saturated soils create an easy pathway for the groundwater movement, thereby enhancing the probability of contamination of the geoenvironment [48, 49, 186–188]. To counter this scenario, many a times, *immobilizing agents* [4], tested for their *sorption and desorption characteristics,* are employed [108, 126, 128, 129]. Usually, *batch tests* are conducted to achieve this, but due to high liquid to solid ratios, these tests fail to simulate real-life situations. Also, these tests fail to come up with recommendations regarding selection of the most suitable and general isotherm, which would

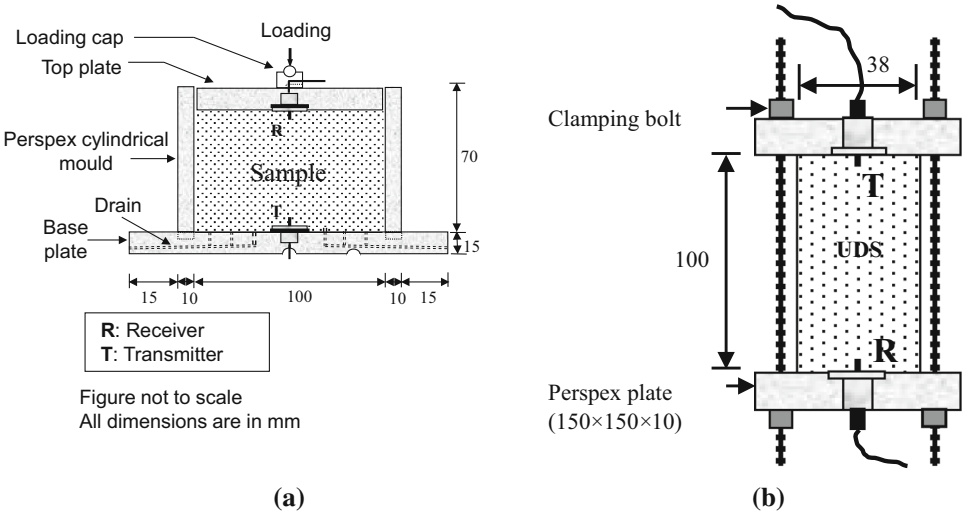

Fig. 24 The test setups used for **a** remolded and **b** undisturbed samples

describe *sorption and desorption characteristics* of geomaterials, precisely [4, 126, 127, 129]. This necessitates determination of the *sorption–desorption* characteristics of geomaterials by conducting 'column tests.' However, due to extremely low hydraulic conductivity of the geomaterials, column tests would require large durations to yield results and hence *geotechnical centrifuge modeling* has been conducted [13, 176, 177].

The setup depicted in Fig. 25 was employed for determining hydraulic conductivity of the sample. This setup, when spun in a geotechnical centrifuge, simulates a *conventional falling-head permeability test* in an accelerated environment. The difference between the hydraulic conductivity tests and the column tests, which facilitate *contaminant-geomaterial* interaction, in a controlled manner, is that for performing the later, the inner cylinder was filled with the *model contaminant*. The contaminants could be different ionic solutions in their active (radionuclides) and/or *inactive* forms. Hence, with the help of the setup depicted in Fig. 25, the *sorption* characteristics of the *contaminant* on *geomaterial* could be established. Subsequently, when the *contaminant* in the inner cylinder is replaced by the distilled water, the *desorption* characteristics of the *contaminant-geomaterial* interaction could be simulated and monitored.

Subsequently, the experimental results can be employed in STANMOD (https://www.ars.usda.gov/pacific-west-area/riverside-ca/us-salinity-laboratory/docs/stanmod-model/), to establish the break-through curves, BTCs, which represent the variation of normalized concentration of the contaminant in the fresh water with respect to time, which quantify *contaminant-geomaterial* interaction for a given contaminant and the geomaterial. In Fig. 26a, IC-1, IC-2 and IC-3 correspond to 8-, 10- and 14.5-mm-thick Israeli chalk sample, centrifuged at 125 g, 100 g and 69 g, respectively. It can be noted from Fig. 26a that for these samples, C_t/C_0 (where C_0 is the initial concentration of the contaminant and C_t corresponds to the concentration of the effluent after time, t) attains almost unity after 62 h, 67 h and 88 h of centrifugation time, respectively. This time, denoted as t_{eq}, corresponds to the dynamic equilibrium sorption state of the material. Furthermore, it can be observed from Fig. 26a that initial BTCs get exhibited only after 3 h, 5 h and 12 h of centrifugation for samples IC-1, IC-2 and IC-3, respectively. This indicates that the time, t_i, required for initial breakthrough to occur depends, apart from the retardation coefficient of the sample (material), on its length, L, and acceleration level, N. Further, in order to obtain t_i for 1-m-thick rock mass, under normal conditions (i.e., $N = 1$), the concept *modeling of models* was employed. The intercept of t_i-N trend, depicted in Fig. 26b, on the ordinate ($N = 1$) is found to yield $t_i = 236{,}113$ h (i.e., 27 years). This demonstrates the utility of the geotechnical centrifuge (also known as accelerated physical modeling) modeling, for simulating and modeling *sorption–desorption* mechanisms, in an extremely short duration.

From this study, it has been demonstrated that the scale factors for the sorption and desorption times are 1.0 and 0.5, respectively. It is believed that the sorption and desorption parameters, obtained from the centrifuge modeling, can be employed for evaluating the efficiency and suitability of immobilizing agents and suitability of the geological formations (repositories), where the toxic/radioactive waste should be disposed.

In order to determine the presence and concentration of contaminants in geomaterials, a contaminant detector (refer Fig. 27) has been developed by Rajeev and Singh [135] and Kumar and Singh [101]. This detector helps in assessing the movement of contaminant front in a soil column (refer Fig. 28). The movement of the *contaminant front* is done by sending a low-frequency sinusoidal signal

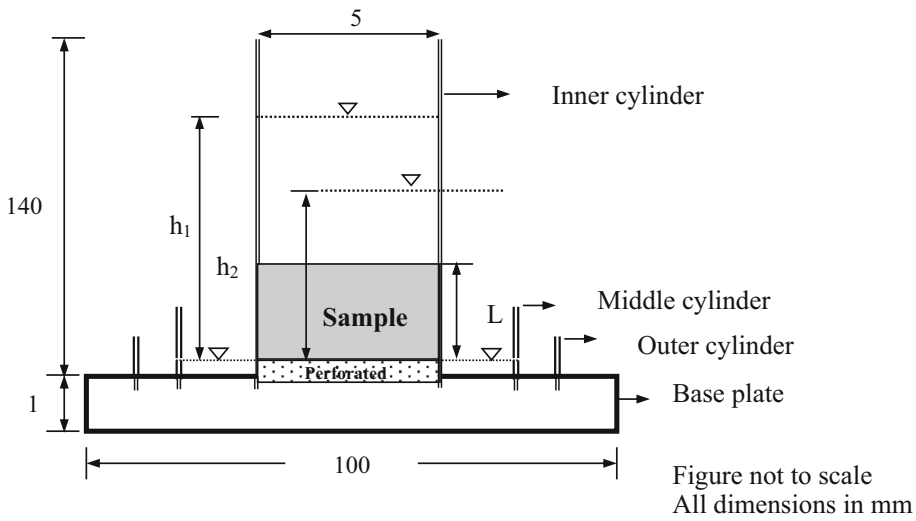

Fig. 25 The setup employed for conducting column tests

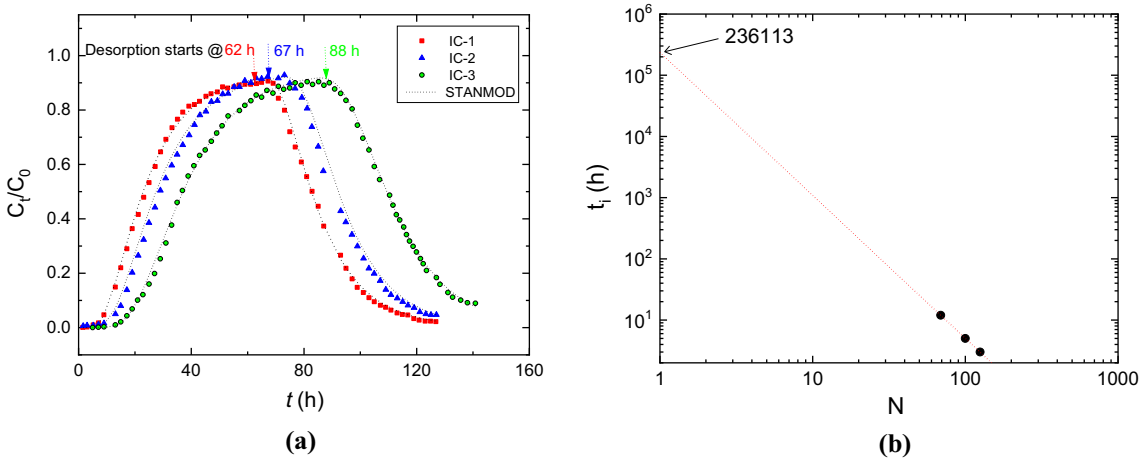

Fig. 26 **a** The BTCs for different samples. **b** Modeling of t_i for the sample

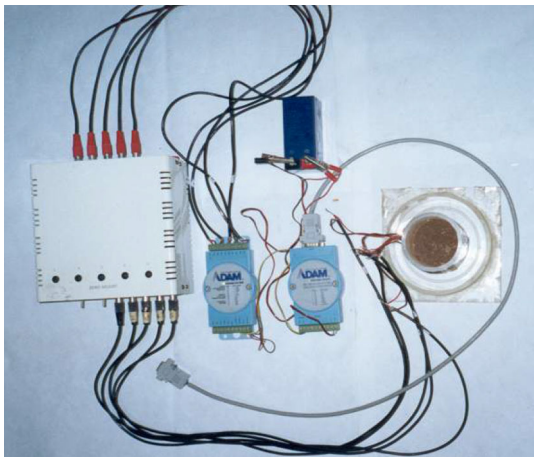

Fig. 27 The soil-contaminant detector

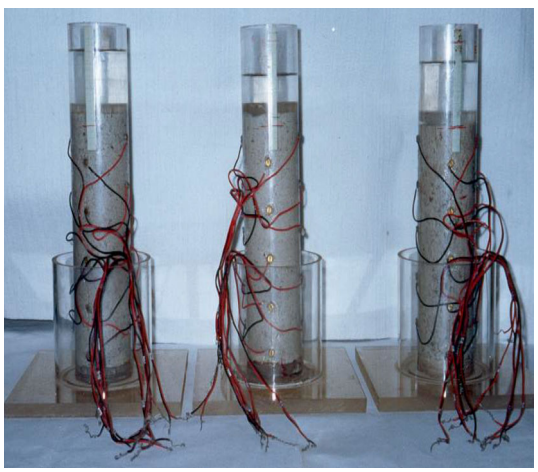

Fig. 28 The soil columns with contaminant placed at their top

into the sample, which is connected to one arm of a Wheatstone's bridge. Hence, with the help of the contaminant detector, concentration of the contaminant at different locations (where electrode pairs are placed, diametrically opposite to each other) along the length of the sample can be detected [101, 102].

Furthermore, to study the mechanism(s) of contaminant transport in the rock mass, viz., diffusion and/or advection, investigations were conducted by Gurumoorthy and Singh [48–50] and Witthüser et al. [223] by using different ions in their *active* (radionuclides) and *inactive* forms. Diffusion cells, depicted in Fig. 29a, b, were developed for monitoring and establishing the response of the intact and fractured rock samples, respectively. Incidentally, Rao and Singh [141] modified the diffusion cell depicted in Fig. 29a to accelerate the *contaminant-geomaterial* interaction that results in *diffusive contaminant transport*. This diffusion cell, refer Fig. 30, enhances the ionic diffusion through the rock sample by applying a suitable electric field across it.

Furthermore, Sreedeep and Singh [192] fabricated a diffusion cell (refer Fig. 31), for investigating the *contaminant-geomaterial* interaction when diffusive contaminant transport occurs in unsaturated soils. The BTCs have been obtained by conducting the impedance spectroscopy, IS [139, 140]. This nondestructive and noninvasive technique has been found to be an excellent way of studying contaminant transport in unsaturated soils.

However, for establishing diffusion characteristics of the saturated and unsaturated soil mass, Rakesh et al. [137] have employed the diffusion cell, depicted in Fig. 32, with sampling ports placed at regular distance on the surface of the cells. These simple studies, which employ indigenously developed diffusion cells, are found to be quite handy for preparing guidelines for safe disposal of the radioactive waste in the geoenvironment.

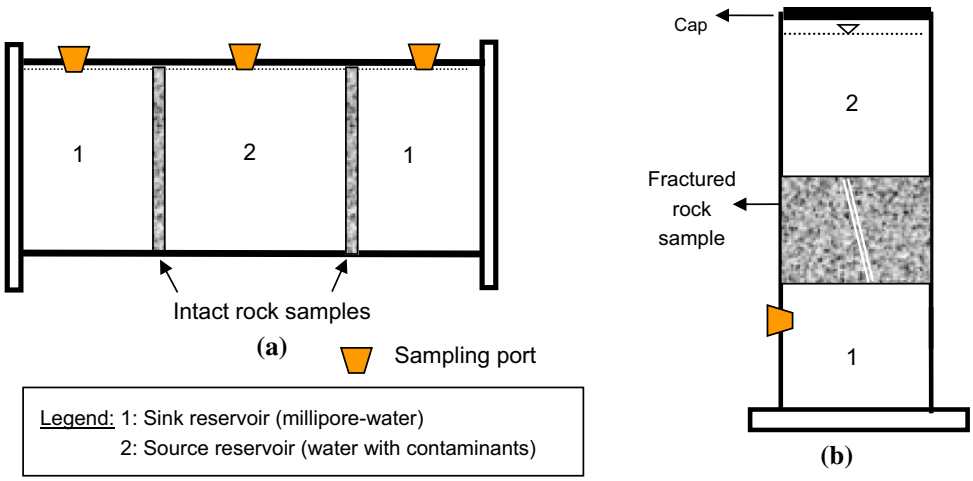

Fig. 29 The diffusion cell for the **a** intact rock sample and **b** fractured rock sample

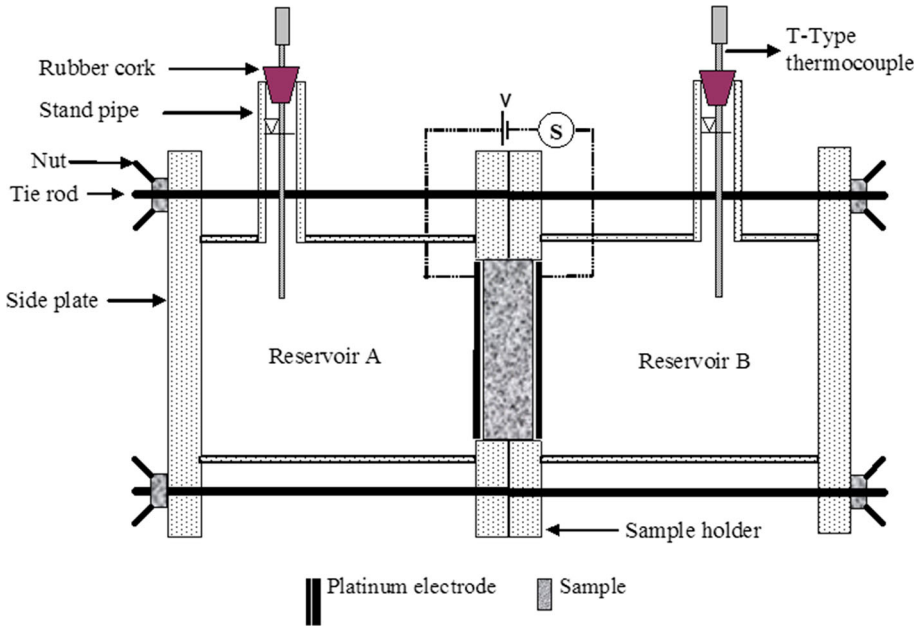

Fig. 30 The diffusion cell for accelerated tests on intact rock samples

Monitoring and Simulation of Heat Migration

As discussed earlier, *contaminant-geomaterial* interaction might also result in generation of heat, mainly due to the chemical reactions. A good example of such a situation is the MSW in landfills, wherein several chemical reactions keep occurring. Furthermore, situations like waste from nuclear and thermal power plants, underground crude oil storage tank, oil-carrying pipelines, air-conditioning ducts, buried conduits and electrical cables, geothermal energy piles, furnaces, boiler units, forging units, brick kilns, solar pond and rocket launching pads [109], necessitate understanding the influence of heat energy on geomaterials [227]. Moreover, remediation of the contaminated land and the thermal stabilization of the soil mass and sludge sediments, underground explosions and natural freeze–thaw cycle persistently subject the migration of thermal energy in geomaterials (the soil and rock mass). Incidentally, the activities like agriculture, wherein the yield can be accelerated by employing a set of parallel buried pipes as a heating system, also induce heating of the soil mass. In all these situations, it becomes mandatory to measure the rate and extent of heat migration in the soil mass. This can be obtained by establishing the thermal regime, i.e., the temperature and heat flux profiles for a prolonged duration, with the help of *sensors,* viz., single needle probe, dual-probe heat pulse (DPHP) and flux sensors [115, 116]. The knowledge of thermal response of geomaterials also has a major role to play in safe and appropriate design of the underground thermoactive structures [1, 57].

In this context, efforts made by earlier researchers toward the development of various techniques, viz., flux

plate method, calorimetric, gradient and combination, guarded hot plate, divided bar apparatus, cylindrical configuration, in situ sphere, heat meter, thermal cell, thermal probe method [112], are worth appreciating. The MEMS (microelectro-mechanical system)-based thermal sensor and differential scanning calorimeter, which are applied to sense the thermal response (say thermal properties) of the soil mass, viz., thermal conductivity, resistivity, diffusivity and volumetric heat capacity, are also being used. Though these methods and techniques are being used by the researchers and practitioners for thermal characterization of geomaterials to understand its heat migration capability, they are time-consuming, complex, tedious and costly. Also, moreover, these methods and techniques do not imbibe the influence of microbial activities, organic content, mineralogical characteristics and heterogeneity of the geomaterials and the MSW. It should be noted that most of these attributes of the geomaterials are sensitive to temperature and hence would have a definite influence over their thermal response, mostly at temperatures different than that prevailing at the ambiance. This calls for extensive studies to establish the mechanism of heat migration in geomaterials, by measuring their thermal response, i.e., thermal regime, particularly, under variable temperature conditions. One of the ways to achieve this would be to quantify 'the zone of influence of the heat source,' by measuring the thermal flux, ϕ, and temperature, θ, over prolonged durations in the spatial domain [110, 111, 113]. This could be done quite efficiently with the help of flux sensors and MEMS-based temperature sensors [203], of extremely high precision.

As depicted in Fig. 33, the test setup for studying heat migration in soil mass consists of a mold, a hot air gun for inducing heat to the sample and a thermocol box. The hot air gun used in this study was manufactured by STEINEL thermopower, Germany (model HL 2010 E), and it operates from 50 °C to 600 °C. The sample was prepared in a mold of dimension 150 mm × 150 mm × 200 mm. The four sides of the mold were made of 8-mm-thick perspex, and the base was made of a 10-mm-thick aluminum plate. The top face of the mold (refer Fig. 33) was kept open to facilitate the flow of heat flux into the sample. After achieving a certain height of the sample, flux sensors were embedded. It was ensured that the sensing face of these sensors faces the heat gun. A soil cover of 50 mm was ensured on the top-most sensor for its proper functioning. Similarly, beneath the bottom-most flux sensor, a 30-mm-thick layer of soil was maintained, which ensures 1-dimensional heat flow in the system (refer section ABHG in Fig. 34). Subsequently, four thermocouples (T-type) were embedded in the sample to measure the temperature at the locations where heat flux sensors were installed. The response of the soil mass, corresponding to hot air gun temperature, θ_{hg}, 80 °C is depicted in Fig. 35.

Apart from this, simple numerical approach, based on the finite difference method, has also been developed to solve the one-dimensional heat conduction equation, which facilitates establishment of the thermal regime in the soil mass. Also, a unified mathematical framework, ATHERES, has also been developed to estimate thermal regime in the dry soil mass. The proposed approach couples Taylor's series into the governing differential equation of one-dimensional heat conduction [113].

As described earlier, *geomaterial–contaminant* interaction might result in endo- or exothermic reactions and/or a coupled flow, viz., heat-induced moisture and contaminant migration [9, 94, 133]. For conducting such experiments, thermal probes (refer Fig. 36a, b) and a thermal property detector, TPD (refer Fig. 36c), were developed [23, 24, 182]. These probes and the TPD have been found to be very helpful in determining the thermal response, viz., thermal resistivity, thermal diffusivity and effusivity, and specific heat, of different geomaterials, corresponding to different moisture contents and dry densities [23, 24, 41, 42, 93, 95, 97, 174, 175, 184, 197]. Krishnaiah et al. [99] and Das et al. [28, 30] have employed this instrument for determining the porosity of the rock and concrete samples, respectively, very successfully.

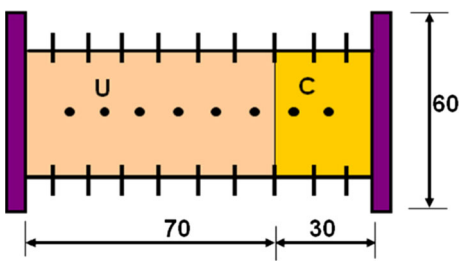

Fig. 31 The diffusion cell developed by Sreedeep and Singh [192]

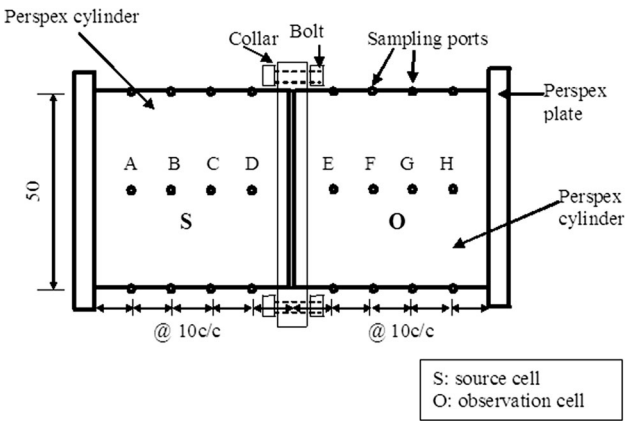

Fig. 32 The diffusion cell developed by Rakesh et al. [137]

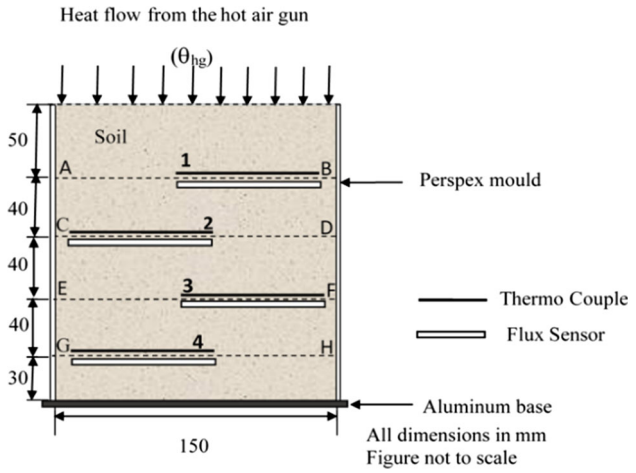

Fig. 33 Details of the test setup

Incidentally, heat migration in soil mass was simulated and monitored, in a geotechnical centrifuge (refer Fig. 37), by Manthena and Singh [105] and Krishnaiah and Singh [96, 98], and the validity of 'modeling of models' for heat migration in soils has been demonstrated, successfully. This study also demonstrated that the geotechnical centrifuge can be used as a research tool to model heat migration in geomaterials.

These studies are a good testimonial of the fact that cost-effective and indigenously made, simple looking devices, viz., thermal probes and TPD, can be utilized for determining thermal properties of geomaterials such as thermal resistivity, thermal diffusivity and specific heat, which are *must to determine* for proper design and safe execution of the projects mentioned above. Such in-house developments also facilitate in demonstrating the facts: (a) thermal resistivity of geomaterials decreases as their dry density and the moisture content increase, (b) the fine-grained soils exhibit higher thermal resistivity as compared to their counterparts, the coarse-grained soils, (c) thermal diffusivity of the geomaterials is found to be practically independent of their dry density, (d) thermal diffusivity of the coarse-grained soils, which is maximum corresponding to the optimum moisture content, is higher than the fine-grained soils, for which the influence of the molding moisture content is practically negligible.

However, these developments should be employed, and if required augmented, for their applications to investigate (a) thermal response of multi-phase geomaterials, viz., frozen geomaterials, gas hydrates and MSW, and (b) coupled phenomenon, wherein the moisture migration occurs due to the imposed thermal gradients.

Role of Environmental Stresses: Genesis of Unsaturated Geomaterials

Depending upon the severity of the *environmental stresses*, geomaterials might experience *moisture loss*, *movement* and/or *redistribution* within. These mechanisms are responsible for geomaterials to acquire *unsaturated-/partially/variably saturated* state. This state of geomaterials is, primarily, dictated by the *suction* present in them. The variation of suction with the water content is commonly known as the soil–water characteristic/retention curve, SWCC/SWRC. A tensiometer, as depicted in Fig. 38, can be employed for soil suction measurement [180, 193, 194]. However, to overcome the limitations associated with the tensiometer measurements, which are limited to $\approx$ 100 kPa, Thakur and Singh [208] and Thakur et al. [209, 210] have developed a methodology, which facilitates measurement of suction up to a few mega-pascal. Subsequently, several methodologies were developed for measuring suction of the soil mass [52, 59–61, 78, 125, 191].

Unsaturated properties of the soil mass such as water retention and hydraulic conductivity also control the contaminant migration in it [179, 180, 185]. Earlier studies reveal that these characteristics mainly depend on the mineralogy, water content, dry density and degree of saturation of the soil [123, 143]. With this in view, various in situ, laboratory techniques, empirical relationships and pedo-transfer functions (PTFs) have been developed by the researchers to establish soil–water characteristic curve, SWCC [62, 158, 196, 209–211]. However, these techniques are tedious, time-consuming, soil specific, require expensive experimental setups and resort to destructive and invasive techniques for determining soil moisture content [194]. Also, most of these techniques suffer particularly in regeneration of the in situ soil conditions and boundary conditions, in an exceptionally small model [18]. Usually, the SWCC is employed for estimating hydraulic

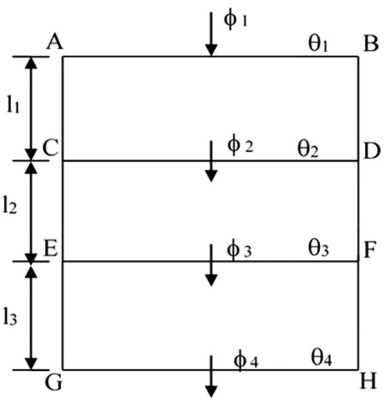

Fig. 34 Details of various sections of the sample

conductivity of the unsaturated soil mass. Hence, techniques that would be helpful in (a) creating the unsaturated state of the soil mass and (b) determination of the unsaturated hydraulic conductivity of the soils, under laboratory and field conditions directly, were developed, as described below.

Laboratory Simulation of Unsaturated State of Geomaterials

The first step in this direction would be to create unsaturated state of the soil mass by (i) employing a geotechnical centrifuge, (ii) imposing thermal flux and (iii) employing a pressure membrane extractor (PME), and determining its instantaneous moisture content by conducting electrical measurements (i.e., voltage across two points in the soil mass). The utility of these techniques for establishing the SWCC easily and that too in a nondestructive and noninvasive manner has been demonstrated [51, 52, 142].

By Centrifugation

The test setup depicted in Fig. 39 was fabricated to attain an unsaturated state of the sample, by centrifugation, followed by establishing the SWCC. As depicted in the figure, point electrodes were fitted diagonally opposite to each other and the voltage across each pair of electrodes, V, was measured by employing the soil conductivity meter developed by Rajeev and Singh [135].

The soil sample (in a slurry form) was poured into the perspex cylinder and later centrifuged for different centrifugation efforts (time and g-level, designated as N). Due to centrifugation, water drains out of the sample and it acquires the *unsaturated* state. At the end of each centrifugation effort, the setup was taken out of the centrifuge and voltage, V, across different electrode pairs was measured. Later, a stainless steel ring was used for retrieving a specimen of the soil for measuring its suction, ψ, by employing a dewpoint potentiameter, WP4 [158]. Subsequently, the ring containing the soil specimen was placed in an oven to determine its moisture content, w. Figure 40a depicts the variation of the measured voltage, V, across electrode pairs A–A, B–B and C–C, with time, t. For the sake of brevity, results of $N = 530$, only, are being presented. It can be observed from the trends depicted in the figure, V decreases as t increases, which indicates that the resistance of the soil mass increases, due to the expulsion of water as a result of enhanced centrifugation efforts. This observation further indicates that soil mass achieves certain unsaturated state after each centrifugation [133, 179, 184, 185]. It was also observed that the difference between the values of V corresponding to a given time between two electrode pairs decreases for higher values of N. This indicates that centrifugation at higher N creates a uniform state of moisture in the sample in a short duration of time. The results have been employed for developing the soil–water characteristic curve, $SWCC_{(Cent)}$, using the Fredlund and Xing [36] best fit. Further, to demonstrate the utility of the proposed technique, the obtained $SWCC_{(Cent)}$ was compared vis-à-vis the SWCCs reported by researchers [158], $SWCC_{(PME\text{-}WP4)}$, and obtained from the pedotransfer function, PTF, proposed by Fredlund et al. [37, 38], $SWCC_{(PTF)}$, as depicted in Fig. 40b. A reasonably good match between the $SWCC_{(Cent)}$ and $SWCC_{(PME\text{-}WP4)}$ can be noticed.

By Imposition of Thermal Flux

The test setup depicted in Fig. 41 was fabricated, as an alternative to the setup depicted in Fig. 39, to create

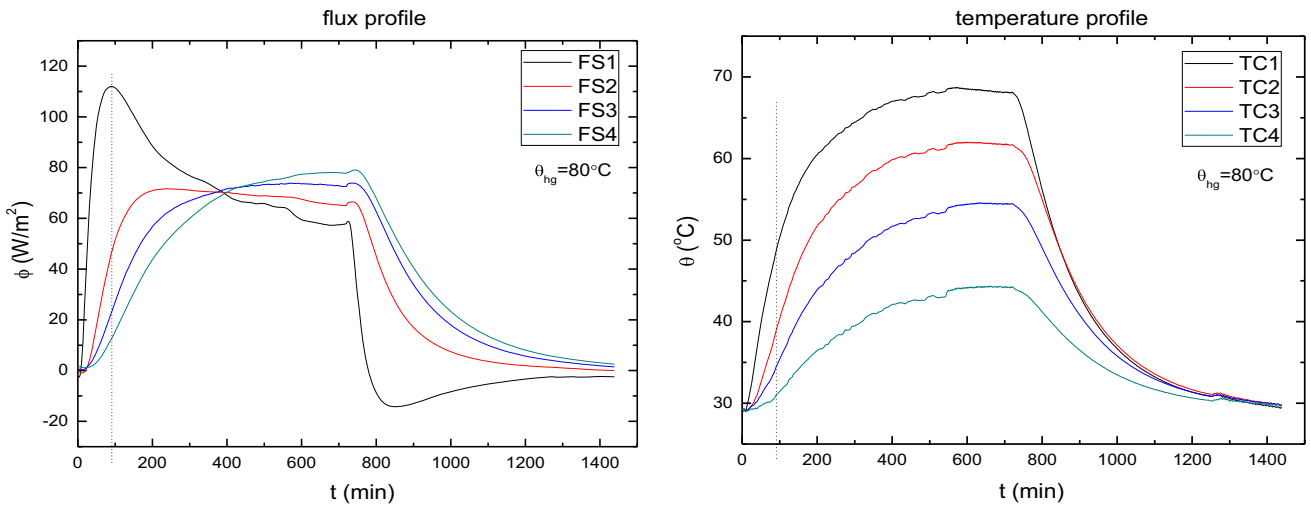

Fig. 35 The variation of thermal flux and temperature, with time in the sample

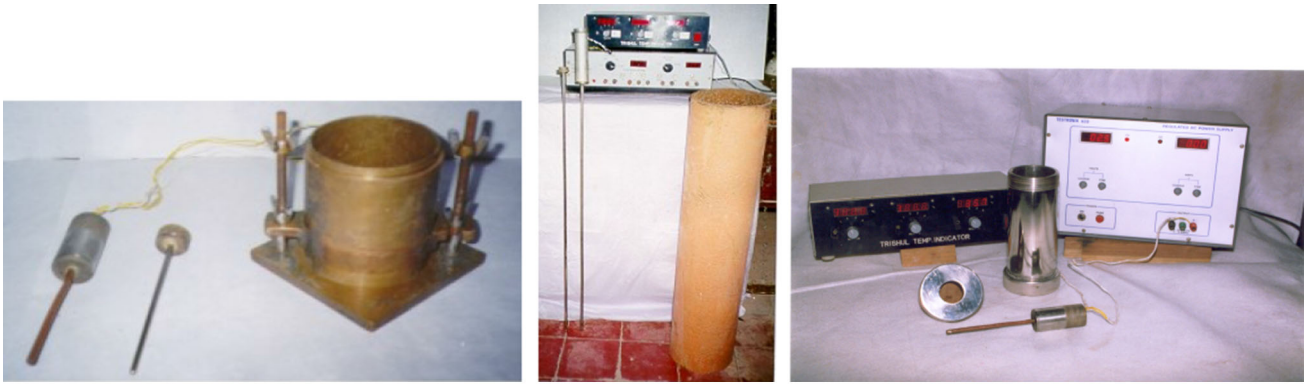

(a) (b) (c)

Fig. 36 The **a** laboratory and **b** field thermal probes and **c** thermal property detector

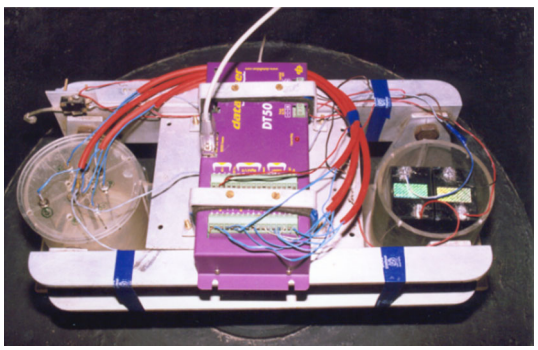

Fig. 37 Instrumentation for heat migration in soils (centrifuge tests)

unsaturated samples and for establishing the SWCC. The *laboratory thermal probe* is the most important part of this setup.

The curved surface of the inner cylinder is perforated in the radial direction. Due to imposition of the thermal flux, water from the soil sample permeates through these perforations and gets collected in the outer cylinder. The electrodes that are fitted on top and bottom plates facilitate measurement of the V with the help of a soil conductivity meter. Also, the cover plate has been provided with four 3-mm-diameter holes for fitting thermocouples, which are placed at different radial distances from the probe. Figure 42a depicts the variation of temperature, θ, and measured voltage, V, with time, t, obtained by imposing a heat flux, Q, of 59.5 W/cm, through the thermal probe.

It can be observed from Fig. 42a that θ varies with time, t, and the maximum temperature built up in the soil mass is about 30 to 40 °C (except for the surface of the probe on which temperature rise is up to 50 to 60 °C). It can also be noticed that, as expected, the rise in θ is least for the thermocouples located at higher radial distances, for a given t. Trends depicted in Fig. 42b indicate that in general, V decreases with an increase in t. This phenomenon can be attributed to the increase in resistance of the soil mass, due to thermal flux-induced moisture migration and hence creation of its unsaturated state. Subsequently, w and ψ for different values of V were computed, and the results are presented in Fig. 43. These data can be employed for developing the soil–water characteristic curve due to thermal flux, $SWCC_{(TF)}$, using the Fredlund and Xing [36] best fit. Further, to demonstrate utility of the proposed technique the $SWCC_{(TF)}$ was compared vis-à-vis the SWCCs reported by researchers [158], $SWCC_{(PME\text{-}WP4)}$, and obtained from the pedo-transfer function proposed by Fredlund et al. [37, 38], $SWCC_{(PTF)}$, as depicted in Fig. 43. A reasonably good match between the $SWCC_{(TF)}$ and $SWCC_{(PME\text{-}WP4)}$ can be noticed from this figure.

By Employing Pressure Membrane Extractor (PME)

The PME unit, employed for creating different moisture states of the specimen, works in the pressure range of 0–1500 kPa and consists of a stainless steel pressure chamber and a base plate, refer Fig. 44.

Four PVC rings (60 mm internal diameter and 20 mm height) were used as specimen holders. These rings contain two pairs (1-1 and 2-2) of stainless steel point electrodes of 2 mm diameter, located diagonally opposite to each other. This arrangement helps in measuring voltage across two points, V, in the soil specimen. Subsequently, as explained earlier, its moisture content, W, was also determined. However, this technique yields the response of the soil mass only up to the applied pressure, which is equal to suction, $\psi \leq 1500$ kPa. Hence, the utility and efficiency of these three techniques for establishing the SWCC have been demonstrated. The most important feature of these techniques is that just by measuring the voltage across two points in the soil mass, its SWCC can be established, quite easily, and that too in a nondestructive and noninvasive manner. It is recommended that extensive experimentations should be conducted to generalize the suitability of the

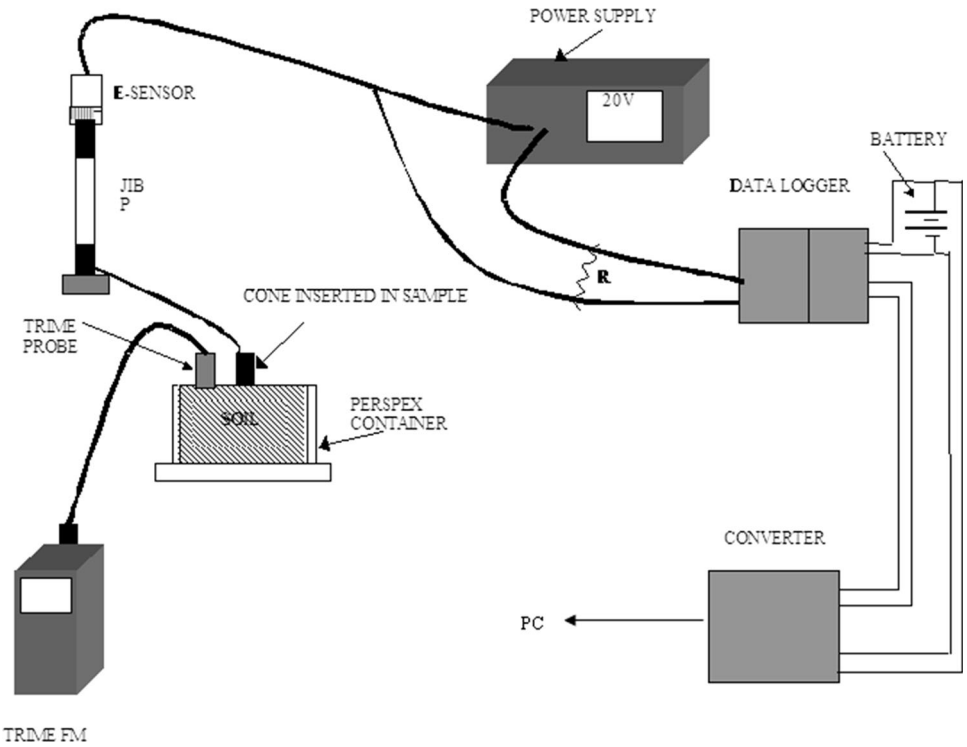

Fig. 38 Details of the instrumentation for measuring soil suction by employing a tensiometer

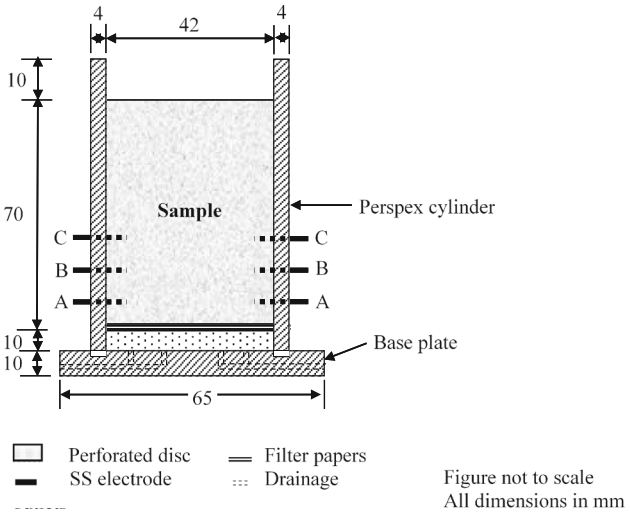

Fig. 39 The setup used for creating unsaturated state of the soil mass by centrifugation

proposed technique for establishing SWCC of different types of soils.

Further, as depicted in Fig. 45, the unsaturated soil hydraulic conductivity, k_u, obtained by employing these three techniques and the PTFs, available in the SoilVision [189] database®, were compared. It must be appreciated that $k_{u(N)}$ are directly measured values, by adopting the methodology proposed by Singh and Kuriyan [180], and not mathematically predicted. It is interesting to note that for all practical purposes, $k_{u(N)}$ of the soil mass does not depend on N.

Hence, it can be said that these methodologies are very useful and handy for establishing the soil–water characteristic curve and for estimating the hydraulic conductivity of unsaturated soils, either directly (in case of centrifugation) or indirectly (i.e., by employing pedo-transfer functions, PTFs).

In Situ Lysimeter

Laboratory column studies (under normal and accelerated gravity environments), numerical modeling and pedo-transfer functions [211] have been employed by the researchers to determine hydraulic conductivity of unsaturated soils [53, 180] and studying contaminant transport [143] in them. However, these methods suffer from several limitations, particularly, as far as regeneration of in situ soil conditions and boundary conditions, in an exceptionally small model, is concerned. Under these circumstances, an in situ lysimeter (Fig. 46, legends used in the figure are explained in the table) has been found to be quite useful for conducting the investigations to obtain hydraulic conductivity of fully or partially saturated soils [53, 143]. A tubular TDR probe has been employed for determining the volumetric moisture content, θ, of the soil as a function of depth, z, by inserting it into access tubes T1 and T2.

Figure 47 depicts spatial variation in the volumetric moisture content, θ, of the soil mass corresponding to

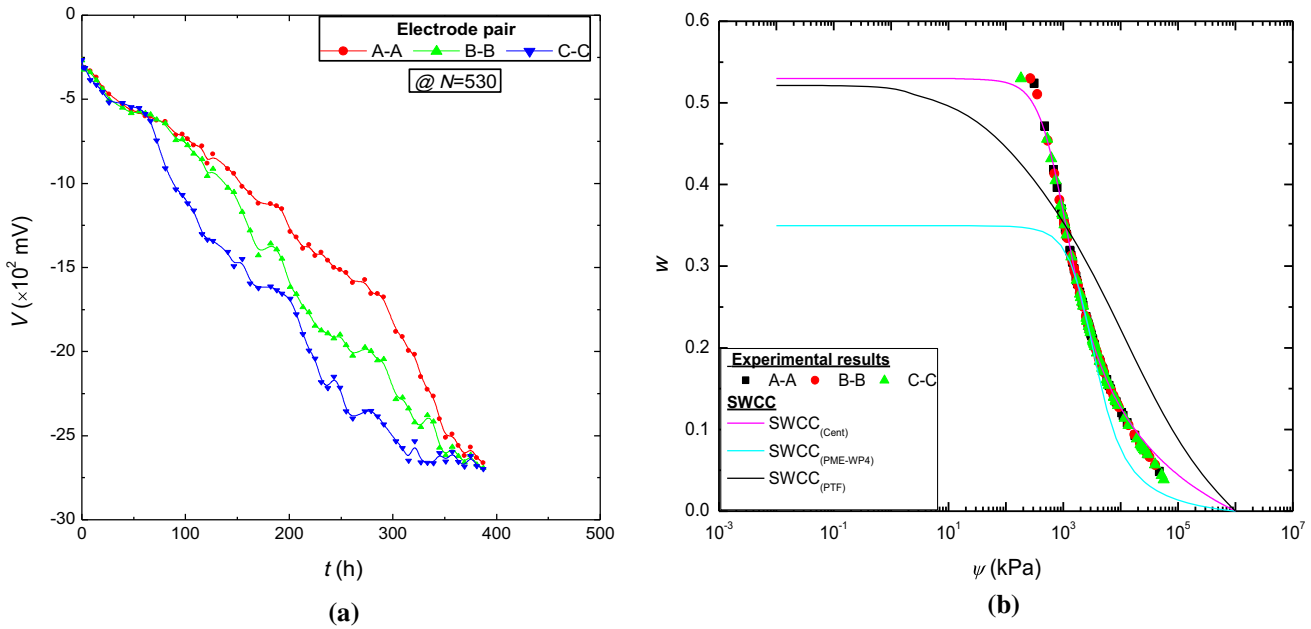

Fig. 40 **a** Variation of the measured voltage across different electrodes with time. **b** Validation of the methodology for obtaining SWCC by centrifugation of the sample

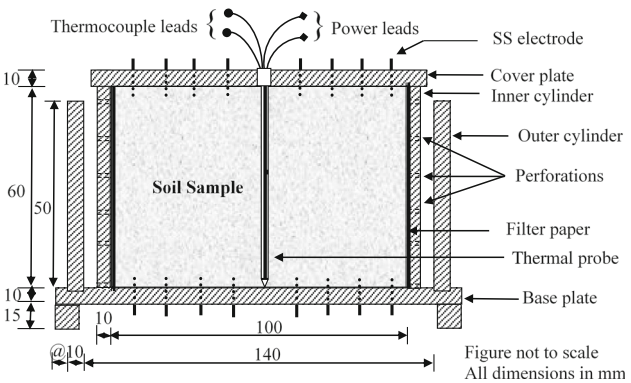

Fig. 41 The setup used for creating unsaturated state of the soil mass by thermal flux imposition

different monsoon seasons (full-monsoon, medium dry and dry seasons). Trends depicted in Fig. 47a show that θ varies over a wide range from 5%, during the fully dry season to 45%, during the full-monsoon season, which correspond to retention and saturation capacity of the soil mass, respectively. It can also be noticed from Fig. 47a that θ increases with depth z. However, a significant scatter in θ values can be observed for $z < 300$ mm, only. Further, since unsaturated soil hydraulic conductivity, k_u, is a function of suction, ψ, efforts were made to determine suction of the soil mass in the lysimeter ψ_f by employing SWCC, with the help of Fredlund and Xing [36] fitting function, to the corresponding measured θ values, as depicted in Fig. 47b. Hence, by knowing ψ_f, k_u was computed by using the PTF proposed by Fredlund et al. [39], as depicted in Fig. 47c.

Role of Environmental Stresses: Cracking of Fine-Grained Soils

The cracking of fine-grained soils can be attributed to the loss of moisture, as a result of its exposure to severe *environmental stresses*, as discussed above. These conditions might cause a nonuniform distribution of moisture and temperature, which might result in an imbalance of the internal energy. The loss of moisture from the fine-grained soils results in their shrinking and subsequently cracking, if they are restrained from undergoing volumetric changes, termed as shrinkage. It has been observed that *cracking* of the fine-grained soils influences its overall engineering behavior (in particular the hydraulic conductivity, consolidation, compressibility and shear strength characteristics). Hence, it becomes mandatory to investigate the mechanism(s) of soil cracking and the parameters that influence it significantly.

In this context, several experimental techniques, viz., triaxial tests, direct tensile tests or suction measurements, have been developed and employed by earlier researchers to measure the tensile strength of fine-grained soils [219] and to study their cracking characteristics [124, 212, 213]. However, these studies yield results that are soil specific and dependent on the methodology adopted. Apart from this, due to the bulk form of the sample, the sample

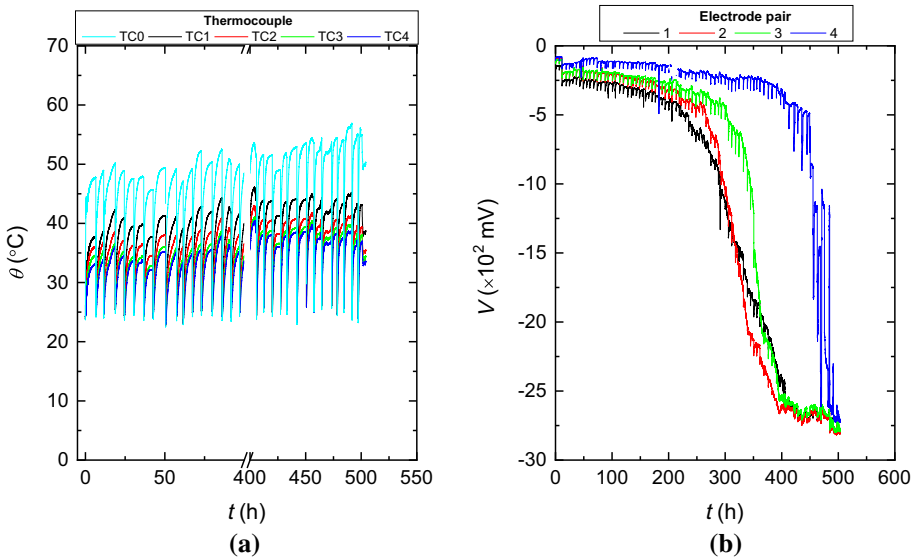

Fig. 42 The variation of **a** temperature and **b** voltage across different electrodes, due to imposition of thermal flux

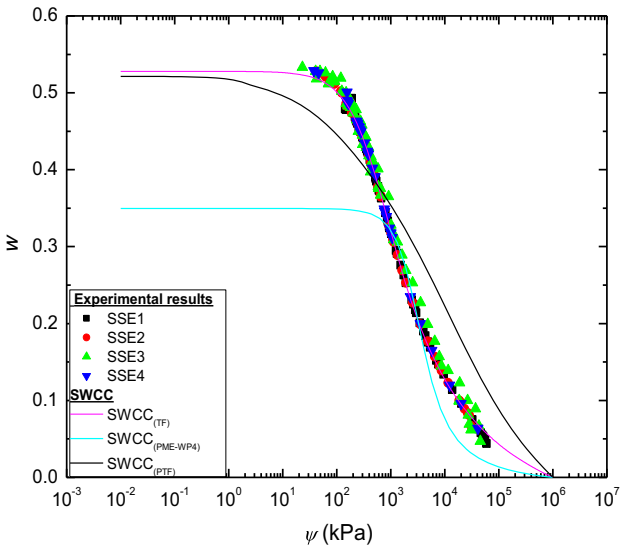

Fig. 43 Validation of the methodology for obtaining SWCC by imposition of thermal flux on sample

heterogeneity (i.e., both in terms of the density and the moisture content) influences test results to a great extent. Under this situation, and in the absence of guidelines regarding sample thickness, determination of the tensile strength of expansive clays by employing their thin samples (1 mm to 5 mm) appears to be an excellent alternative. Efforts have been made to determine *tensile strength* of fine-grained soils, by resorting to techniques that deal with measurement of the (a) deflection undergone by a silicon wafer (refer Fig. 48a, b), due to air-drying of a thin film of these clays, with the help of a laser beam [171], and (b) measuring suction by employing a dewpoint potentiameter, WP4 [210]. Results obtained from these techniques were critically evaluated vis-à-vis those obtained from triaxial tests and empirical relationships available in the literature. It has been observed that there is a unique relationship between the results of the thin and thick samples and hence thin samples of expansive clays can be employed for determining their tensile strength [207, 214, 215]. This shows the usefulness of the proposed techniques for measuring the *tensile strength* of the fine-grained that too expansive soils.

The photograph and the schematic of the experimental setup used to measure the tensile stress developed in the thin film are depicted in Fig. 48a, b, respectively. As depicted in Fig. 48b, L1 and L2 are incident and reflected rays, respectively, and X is the displacement of the laser beam on the detector due to certain deflection of the wafer.

Subsequently, X, and stress, σ, as a function of time are recorded for thin film, as depicted in Fig. 49. The stress corresponding to the peak value yields the tensile strength of the specimen.

This methodology of determining tensile strength of fine-grained soils, in tandem with application of dewpoint potentiameter, WP4, for expansive soils, in particular, corresponding to different liquid to solid ratios has been found to be quite useful. Results obtained from these methodologies were critically evaluated vis-à-vis those obtained from the triaxial tests and the empirical relationships reported in the literature. It has been observed that there is a unique relationship between the results of the thin and thick samples. Hence, the proposed methodology can be employed for determining *tensile strength* of the fine-grained soils, just by knowing their mineralogical composition and the water content. However, extensive studies should be conducted on different minerals, and soils of different mineralogical composition to generalize these findings.

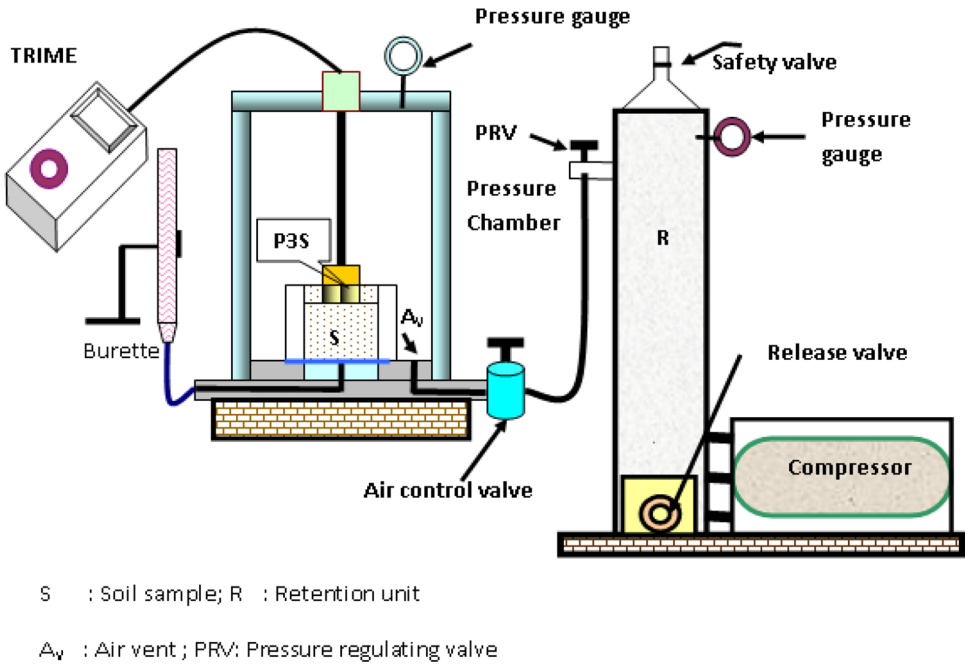

Fig. 44 The setup used for creating unsaturated state of the soil mass by employing a pressure membrane extractor

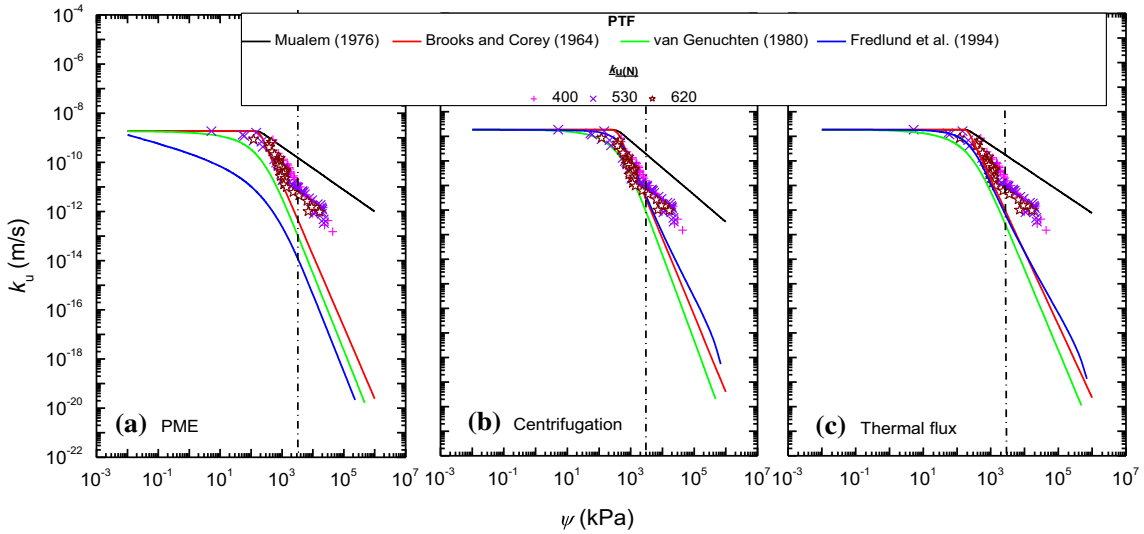

Fig. 45 Evaluation of different techniques employed for estimating unsaturated soil hydraulic conductivity

Concluding Remarks and the Path Ahead

Various instrumentation techniques developed by *THE ENVGEO*s for providing solutions to various geoenvironmental issues have been presented in this paper. These techniques facilitate obtaining appropriate solutions to storage and safe disposal of hazardous and toxic wastes in geomaterials and thus minimizing the adverse effect on the geoenvironment. Though most of these techniques are found to be functioning quite satisfactorily in the laboratory environment, extensive in situ investigations must be carried out that too on different types of geomaterials to demonstrate their robustness and suitability.

Though the (limited) contents of this paper must have successfully highlighted the necessity of *interdisciplinary research* in the field of contemporary geotechnical engineering, the following needs are to be addressed:

1. The impact of *biogeochemical (biomediated)* processes, viz., *decay, degradation* and *upgradation*, that occur in geoenvironment, on *geomaterials*, should be studied and included in the analysis of geotechnical problems. The modification of engineering characteristics of the coarse-grained soils due to *biologically*

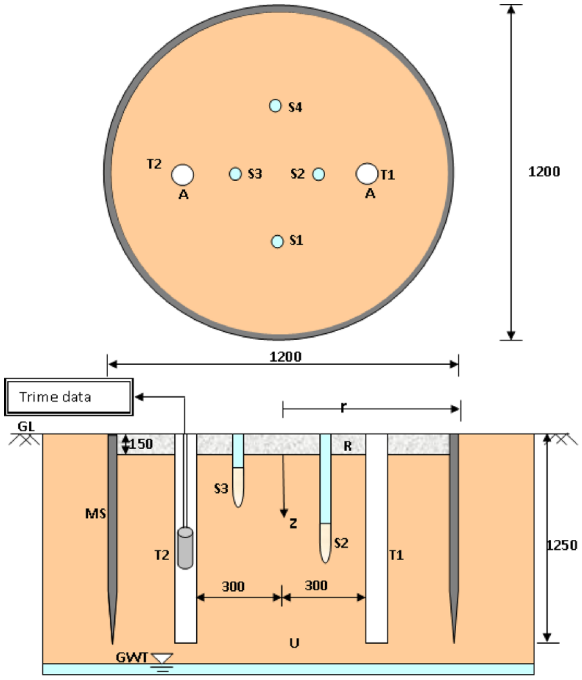

Symbol	Description	Purpose
A	Access tube	Moisture detection probe
GWT	Groundwater table	
R	Spiked soil	To simulate contaminated soil with Tritium
S1	Suction sampler (r,z)	(30, 40)
S2		(10, 30)
S3		(10, 20)
S4		(30, 10)
MS	Mild steel ring	For creating a control volume of approximately 1 m^3
T1 & T2	Access tubes for TDR probe	For determining in-situ moisture content of the control volume
U	Undisturbed soil	Control volume of the soil

Fig. 46 Details of the in situ lysimeter

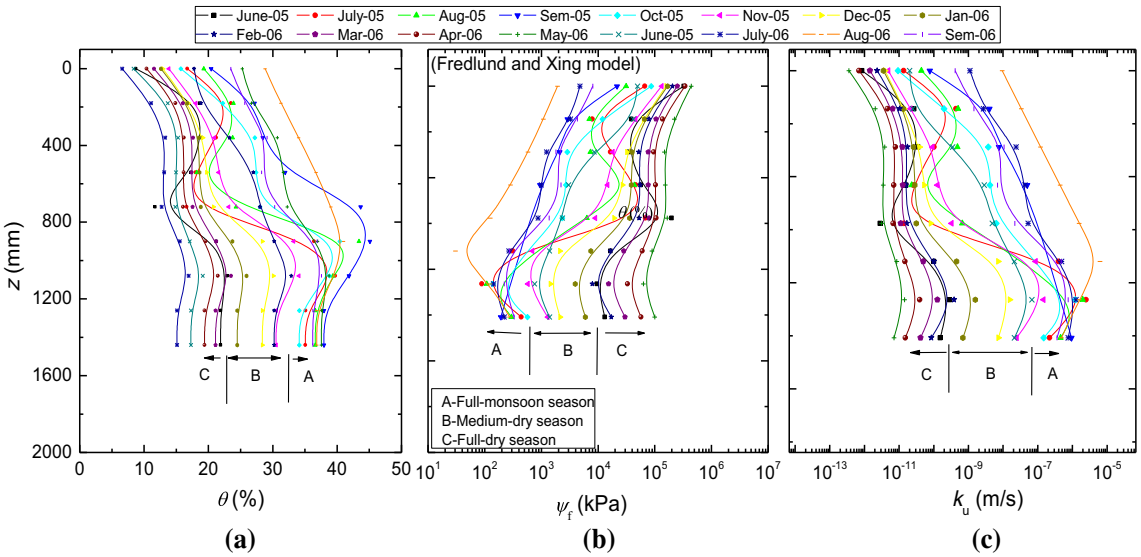

Fig. 47 The variation of **a** volumetric moisture content, **b** suction and **c** k_u, with z for different monsoon seasons

induced mineralization is an excellent example, in this context.

2. The role of *geomaterial* and *pore–fluid* interaction in the soil matrix at the microstructure level to address the *real-life* situations such as offshore landslides, sedimentation, migration of the fines and slurry transportation for various industrial applications, viz., dredging and mineral processing, should be studied. In order to address this, investigations are warranted on the rheological behavior of soil–water systems corresponding to *water content* higher than the *liquid limit* [170].
3. Accelerated decomposition of (a) unsegregated municipal solid waste, MSW, in a bioreactor landfill and (b) organic content rich soils, should be studied extensively, in line with the philosophy, *waste to energy*. Also, pilot-scale studies to incorporate the

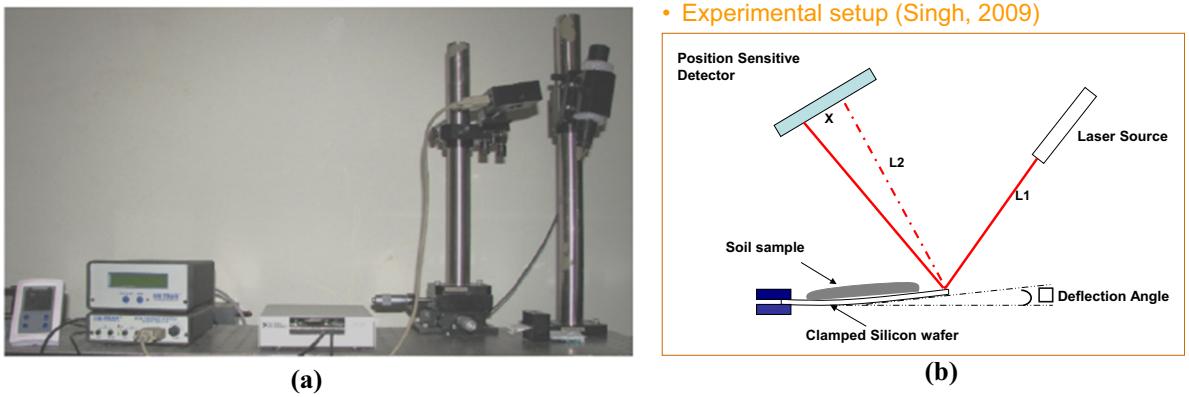

Fig. 48 **a** The experimental setup. **b** The basic concept of the tensile strength determination

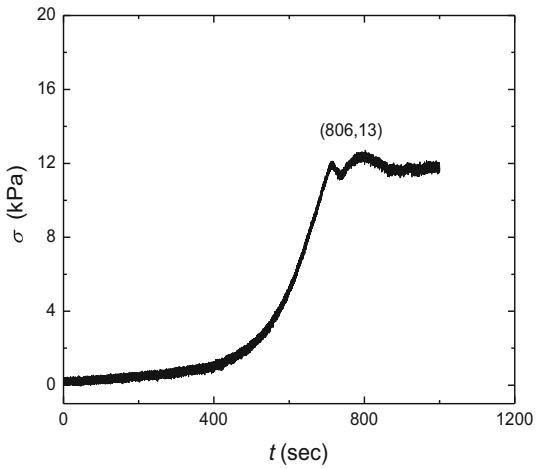

Fig. 49 Experimental results depicting the variation of stress with time for a thin clay specimen

effect of *heterogeneity* on various *physico-biochemical* properties associated with these geomaterials, with the help of *sensors* and *probes*, should also be attempted. Apart from the laboratory and field investigations, numerical modeling related to *coupled processes* that are responsible for decomposition of these geomaterials must be attempted [148]. Attempts should also be made to utilize the nondegradable fraction of the residues, which is a source of refuse-derived fuel, RDF, from the MSW.

4. The MSW *landfill mining*, a precursor to their *rehabilitation* and *reclamation of the derelict land*, is shaping up as a giant 'techno-socio-economical' issue, which should be handled with great diligence. However, it should be realized that the *landfill mining* would result in extreme volumes of the *landfill-mined residues* and subsequently their handling, segregation, storage, transportation and utilization for development of *infrastructure* and *soil conditioning* need to be addressed scientifically. Appropriate *standards, guidelines and policies* need to be developed in this context.
5. The industrial by-products, IBPs, viz., bauxite residues, slags, fly ash, mine overburden dumps, tailings, plastics, should be treated as the *man-made resource* for *sustainable development* [149]. This could be attained by developing proper technology(ies) based on extensive R&D for *bulk utilization* of the IBPs. Attempts should also be made toward the *creation and implementation* of appropriate policies. In this context, the *hazard* and *toxicity* zonation of the entire country would be advantageous.
6. Geomechanical modeling of *multi-phase* geomaterials, viz., permafrost, gas hydrates bearing sediments, thermally stabilized soils, the municipal solid waste, which is still in its nascent stage, should be taken up.

However, in order to accomplish such contemporary research, indigenous development of the test setups and paraphernalia, which also falls in line with the Government of India initiative, MAKE IN INDIA, is the dire need of the hour. Furthermore, most of these issues could easily be taken up as *start-ups* by the professionals, who are concerned about the *generations to follow*, and for whom the sky is the limit. This would also remind them that the path ahead is not so easy to tread, but *if they desire to blossom like a rose in the garden, they have to learn the art of adjusting with the thorns*.

I would also like to add here that audiences' critical comments and suggestions are utmost welcome without which it would be difficult for *The ENVGEO*s to march ahead and follow the philosophy *Never stop learning, because life never stops Teaching* …. Furthermore, the outcome of these initiatives should be *adopted*, *challenged* and *improvised* in view of the fact that *Life is a Camera, Focus on what's important Capture the good times,*

Develop from the negatives and if things don't work out, Take another Shot…

Acknowledgements I would like to sincerely thank the *Indian Geotechnical Society* for *selecting me to deliver the 40th IGS Annual Lecture*, which has provided me an opportunity to *introspected* my activities, in the extremely intriguing and enchanting field of *geoenvironmental engineering* [181]. It was indeed a privilege to receive feedback on the philosophy of developing this manuscript from my Gurus (Prof. P. K. Basudhar, Prof. Yudhbir, Prof. C. S. Desai, Prof. M. R. Madhav, Prof. N. S. V. Kameswara Rao and Prof. S. Chandra). This interaction certainly reminded me of the days that I spent at IIT Kanpur as a student and research scholar. As many who had been associated with me have echoed, the unconditional support and motivation that I have received from Mrs. Ritu Singh, my better-half, and Ms. Yashi Singh, my daughter, is beyond describing in words. Help received from Dr. Anjan Patel, Prof. Ashok Kr. Gupta, Dr. Nevin Koshy, Dr. Prabir Kolay and Dr. Vikas Sharma in the entire course of preparation of this manuscript is thankfully acknowledged. My research group (Shashank, Rakshith, Ganaraj, Arif, Chandana, Lijith, Bhini, Goli Venkata, Himanshu and Tushar) deserves a special *thank you* for *motivating* and assisting me in developing this manuscript. I take this opportunity to acknowledge the help and support that I have received from the examiners of theses, (invisible) reviewers and editorial board members of various Journals, which turned out to be a blessing in disguise for *THE ENVGEO*s. The financial help from various funding agencies and industries is also thankfully acknowledged.

References

1. Abuel-Naga H, Raouf MIN, Raouf AMI, Nasser AG (2015) Energy piles: current state of knowledge and design challenges. Environ Geotech 2(4):195–210
2. Abu-Zreig MM, Al-Akhras NM, Attom MF (2001) Influence of heat treatment on the behavior of clayey soils. Appl Clay Sci 20:129–135
3. Akbulut S, Arasan S (2010) The variations of cation exchange capacity, pH, and zeta potential in expansive soils treated by additives. Int J Civ Struct Eng 1(2):139–154
4. Arnepalli DN, Rao BH, Shanthakumar S, Singh DN (2010) Determination of distribution coefficient of geomaterials and immobilizing agents. Can Geotech J 47:1139–1148
5. Arnepalli DN, Shanthakumar S, Rao HB, Singh DN (2008) Comparison of methods for determining specific surface area of fine-grained Soils. Geotech Geol Eng 26(2):121–137
6. ASTM C 204 (1984) Standard test method for fineness of portland cement by air permeability apparatus. Annual Book of ASTM Standards, 04.01, ASTM, West Conshohocken, PA, USA, pp 56–162
7. ASTM D 4646-03 (2008) Standard test method for 24-h Batch-Type measurement of contaminant sorption by soils and sediments. ASTM International, West Conshohocken, Pennsylvania, USA
8. Azizian S (2004) Kinetic models of sorption: a theoretical analysis. J Colloid Interface Sci 276:47–52
9. Bao J, Xu Z, Fang Y (2016) A coupled thermal-hydro-mechanical simulation for carbon dioxide sequestration. Environm Geotech 3(5):312–324
10. Bartake PP, Singh DN (2007) A generalized methodology for determination of crushing strength of granular materials. Geotech Geol Eng 25:203–213
11. Bartake PP, Singh DN (2005) Determination of crushing strength of cenospheres. J ASTM Int 2(7):1–9
12. Bartake PP, Singh DN (2007) Studies on determination of shear wave velocity in sands. Geomech Geoeng Int J 2(1):41–49
13. Bartake PP, Raghunandan S, Singh DN (2006) Modelling liquefaction of sand in a geotechnical centrifuge. J South East Asia Geotech Soc 11:131–135
14. Bartake PP, Patel A, Singh DN (2008) Instrumentation for bender element testing of soils. Int J Geotech Eng 2(4):395–405
15. Bathija AP, Liang H, Lu N, Prasad M, Batzle ML (2009) Stressed swelling clay. Geophysics 74(4):A47–A52
16. Bayat H, Ebrahimi E, Ersahin S, Hepper EN, Singh DN, Amer AMM, Yukselen-Aksoy Y (2015) Analyzing the effect of various soil properties on the estimation of soil specific surface area by different methods. Appl Clay Sci 116–117:129–140
17. Bhat AM, Rao BH, Singh DN (2007) A generalized relationship for estimating dielectric constant of soils. J ASTM Int 4:1–12. https://doi.org/10.1520/jai100635
18. Borana L, Yin J-H, Singh DN, Shukla SK, Tong F (2018) Direct shear testing study of the interface behavior between steel plate and compacted completely decomposed granite under different vertical stresses and suctions. J Eng Mech ASCE 144(1):04017148
19. Brooks RH, Corey AT (1964) Hydraulic properties of porous medium. Hydrology paper. Colorado State University, Fort Collins, Colorado
20. Chembukavu AC, Mohammad A, Singh DN (2019) Bioreactor landfills in developing countries: a critical review. J Solid Waste Technol Manag. https://doi.org/10.5276/JSWTM.2018.xx
21. Chorom M, Rengasamy P (1996) Effect of heating on swelling and dispersion of different cationic forms of a smectite. Clay Clay Miner 44(6):783–790
22. Cox RJ, Peterson HL, Young J, Cusik C, Espinoza EO (2000) The forensic analysis of soil organic by FTIR. Forensic Sci Int 108:107–116
23. Dalinaidu A, Singh DN (2004) A field probe for measuring thermal resistivity of soils. J Geotech Geoenviron Eng ASCE 130(2):213–216
24. Dalinaidu A, Singh DN (2004) A generalized procedure for determining thermal resistivity of soils. Int J Therm Sci 43(1):43–51
25. Dalinaidu A, Das BB, Singh DN (2007) Methodology for rapid determination of pozzolanic activity of materials. J ASTM Int 4:1–11. https://doi.org/10.1520/jai100343
26. Dangayach S, Singh DN, Kumar P, Dewri SK, Roy B, Tandi C, Singh J (2015) Thermal instability of gas hydrate bearing sediments: some issues. Mar Pet Geol 67:653–662
27. Daphalapurkar NP, Wang F, Fu B, Lu H, Komanduri R (2011) Determination of mechanical properties of sand grains by nanoindentation. Exp Mech 51(5):719–728
28. Das BB, Singh DN, Pandey SP (2008) Experimental revalidation of certain durability design provisions for concrete with reference to the indian code of practice. Cem Wapno Beton XIII/LXXV(1):9–18
29. Das BB, Singh DN, Pandey SP (2011) Rapid chloride ion permeability of OPC and PPC based carbonated concrete. J Mater Civ Eng ASCE 24(5):606–611
30. Das BB, Singh DN, Pandey SP (2008) Some investigations for establishing suitability of Watson's strength-porosity model for concrete. J ASTM Int 5:1–10. https://doi.org/10.1520/jai101345
31. Du YJ, Ning-Jun J, Liu S, Jin F, Singh DN (2015) Physical properties, electrical resistivity and strength characteristics of carbonated silty soil admixed with reactive magnesia. Can Geotech J 52(11):1699–1713
32. Du YJ, Ning-Jun J, Liu S, Jin F, Singh DN, Puppala A (2014) Engineering properties and microstructural characteristics of cement stabilized zinc-contaminated kaolin. Can Geotech J 51:289–302

33. Eisazadeh A, Kassim KA, Nur H (2012) Solid-state NMR and FTIR studies of lime stabilized montmorillonitic and lateritic clays. Appl Clay Sci 67(68):5–10
34. ESP (1976) Electrostatic precipitator manual. The Mcilvaine Company, Northbrook, Illinois, USA
35. Fan RD, Liu SY, Du YJ, Reddy KR, Yang YL (2017) Impacts of presence of lead contamination on settling behavior and microstructure of clayey soil. Appl Clay Sci 142:109–119
36. Fredlund DG, Xing A (1994) Equations for the soil water characteristic curve. Can Geotech J 31:533–546
37. Fredlund DG, Fredlund MG, Wilson GW (1998) Estimation of unsaturated soil properties using a knowledge-based system. In: Proceedings of the 2nd international conference on unsaturated soils, UNSAT'98, Beijing, China, pp 17–30
38. Fredlund DG, Fredlund MG, Wilson GW (1997) Prediction of the soil-water characteristic curve from grain-size distribution and volume-mass properties. In: 3rd Brazilian symposium on unsaturated soils, Rio de Janeiro, Brazil, pp 1–12
39. Fredlund DG, Xing A, Huang S (1994) Predicting the permeability function for unsaturated soil using the soil-water characteristic curve. Can Geotech J 31(3):533–546
40. Ganaraj K, Singh DN (2017) Contemporary issues related to utilization of industrial byproducts. Adv Civ Eng Mater ASTM Int 6(1):444–479
41. Gangadhara Rao MVBB, Singh DN (1999) A generalized relationship to estimate thermal resistivity of soils. Can Geotech J 36(4):767–773
42. Gangadhara Rao MVBB, Kolay PK, Singh DN (1998) Thermal characteristics of a class F fly ash. Cem Concr Res 28(6):841–846
43. Goreham VC, Lake CB (2018) Diffusion and sorption of volatile organic compounds through soil-cement materials. Environ Geotech 5(3):134–145
44. Gumaste SD, Iyer KR, Sharma S, Channabasavaraj W, Singh DN (2014) Simulation of fabric in sedimented clays. Appl Clay Sci 91–92:117–126
45. Gumaste SD, Iyer KR, Sharma S, Singh DN (2014) Determination of the fabric alteration of marine clays. Acta Geotech Slov 11(2):21–31
46. Gumaste DS, Singh DN (2013) Laboratory studies to investigate the influence of thermal energy on soil-fabric. Geomech Geoeng Int J 8(3):209–214
47. Gumaste SD, Singh DN (2010) Application of impedance spectroscopy for determining fabric anisotropy of fine-grained soils. J Test Eval ASTM 38(3):309–318
48. Gurumoorthy C, Singh DN (2004) Diffusion of Iodide, cesium and strontium in charnockite rock mass. J Radioanal Nucl Chem 262(3):639–644
49. Gurumoorthy C, Singh DN (2004) Experimental methodology to assess contaminant diffusion in rock mass. J Environ Monit Assess 91:277–291
50. Gurumoorthy C, Singh DN (2005) Centrifuge modeling of diffusion through the rock mass. J Test Eval ASTM 31(1):562–568
51. Hanumantha Rao B, Singh DN (2010) Application of thermal flux for establishing soil-water characteristic curve of kaolin. Geomech Geoeng Int J 5(4):259–266
52. Hanumantha Rao B, Singh DN (2010) Establishing soil-water characteristic curve of a fine-grained soil from electrical measurements. J Geotech Geoenviron Eng ASCE 136(5):751–754
53. Hanumantha Rao B, Sridhar V, Rakesh RR, Singh DN, Narayan PK, Wattal PK (2009) Application of in-situ lysimetric studies for determining soil hydraulic conductivity. Geotech Geol Eng 27:595–606
54. Hanumantha Rao B, Sridhar V, Rakesh RR, Singh DN, Narayan PK, Wattal PK (2013) Lysimetric studies for modelling radioactive contaminant transport in soils. IJEWM 12(3):318–339
55. Hatten J, Zabowski D, Scherer G, Dolan E (2005) Comparison of soil properties after contemporary wildfire and fire suppression. For Ecol Manag 220(1–3):227–241
56. Hoyos LR, DeJong JT, McCartney JS, Puppala AJ, Reddy KR, Zekkos D (2015) Environmental geotechnics in the U.S. region: a brief overview. Environ Geotech 2(6):319–325
57. Hytiris N, Emmanuel R, Aaen B, Church ES, Campbell DS, Ninikas K, Robertson A (2017) Heat recovery from mine workings: opportunities in the glasgow area. Environ Geotech 4(6):395–401
58. IAEA (2004) Safety assessment methodologies for near surface disposal facilities, results of a coordinated research program, Review and Enhancement of Safety Assessments Approaches and Tools, vol 1. International Atomic Energy Agency, Vienna
59. Iyer KR, Jeevan J, Shetty R, Singh DN (2018) Some investigations to quantify hysteresis associated with water retention behaviour of fine-grained Soils. Geomech Geoeng Int J. https://doi.org/10.1080/17486025.2018.1445872
60. Iyer KR, Joseph J, Lopes BCFL, Singh DN, Tarantino A (2018) Water retention characteristics of swelling clays in different compaction states. Geomech Geoeng Int J 13(2):88–103
61. Jayanth S, Iyer K, Singh DN (2013) Continuous determination of drying-path SWRC of fine-grained soils. Geomech Geoeng Int J 8(1):28–35
62. Jayanth S, Iyer K, Singh DN (2012) Influence of drying- and wetting- cycles on SWCCs of fine-grained soils. J Test Eval ASTM 40(3):376–386
63. Jayanthi PNV, Singh DN (2016) Utilization of sustainable materials for soil stabilization: state-of-the-art. Adv Civ Eng Mater ASTM Int 5(1):46–79
64. Jayanthi PNV, Kuntikana G, Singh DN (2017) Stabilization of fine-grained soils against desiccation cracking using sustainable materials. Adv Civ Eng Mater ASTM Int 6(1):36–66. https://doi.org/10.1520/ACEM20160037
65. Jha B, Singh DN (2011) A review on synthesis, characterization and industrial applications of flyash zeolites. J Mater Educ 33(1–2):65–132
66. Jha B, Singh DN (2012) Zeolitization characteristics of a flyash from wet- and dry- disposal systems. Acta Geotech Slov 2:63–71
67. Jha B, Singh DN (2013) Synthesis of higher grade fly ash zeolite X from fly ash by three step fusion. Mater Perform Charact ASTM 2(1):285–295
68. Jha B, Singh DN (2014) Formation of meso- and micro-pores in fly ash zeolites by three-step activation. Acta Geotech Slov 11(1):63–69
69. Jha B, Singh DN (2014) Quantification of transitions occurring in a hydrothermally activated fly ash. Mater Perform Charact ASTM 3(1):239–254
70. Jha B, Singh DN (2014) A three step process for purification of fly ash zeolites by hydrothermal treatment. Appl Clay Sci 90:122–129
71. Jha B, Koshy N, Singh DN (2015) Establishing two-stage interaction between fly ash and NaOH by X-ray and infrared analyses. Front Environ Sci Eng 9(2):216–221
72. Joseph J, Dangayach S, Singh DN, Kumar P, Dewri SK, Tandi C, Singh J (2017) Investigation on excess gas method for synthesis of methane gas hydrates. J Nat Gas Sci Eng 42:203–215
73. Joseph J, Singh DN, Kumar P, Dewri SK, Tandi C, Singh J (2016) State-of-the-art on gas hydrates and relative permeability of hydrate bearing sediments. Mar Georesour Geotechnol 34(5):450–464. https://doi.org/10.1080/1064119X.2015.1025929
74. Kadali S, Sharma S, Singh DN (2013) Application of nanoindentation to establish influence of heat on soils. Eng Geol 162:14–21

75. Kadali S, Singh DN, Shekhawat SK (2014) Application of X-ray diffraction analysis for determining residual stresses on soil particles due to thermal treatment. J Test Eval ASTM Int 42(5):1240–1247
76. Kadali S, Susha Lekeshmi SU, Sharma S, Singh DN (2013) Investigations to establish the influence of the thermal energy field on soil properties. Acta Geotech Slov 10(2):59–76
77. Kadali S, Susha Lekshmi SU, Singh DN, Maryam Shojaei Baghini MS (2016) Application of heat of wetting for determination of soil specific characteristics of fine-grained soils. J Test Eval ASTM 44(6):2231–2243. https://doi.org/10.1520/jte20150308
78. Kannan IR, Jayanth S, Gurnani S, Singh DN (2013) Influence of initial water content and specimen thickness on the SWCC of fine-grained soils. Int J Geomech 13(6):894–899
79. Kaya A, Ören AH, Yükselen Y (2006) Settling of kaolinite in different aqueous environment. Mar Georesour Geotechnol 24(3):203–218
80. Kaya A, Yukselen Y (2005) Zeta potential of clay minerals and quartz contaminated by heavy metals. Can Geotech J 42(5):1280–1289
81. Ketterings QM, Bigham JM, Laperche V (2000) Changes in soil mineralogy and texture caused by slash and burn fires in Sumatra, Indonesia. Soil Sci Soc Am J 64(3):1108–1117
82. Kolay PK, Singh DN (2000) Effect of zeolitization on compaction, consolidation and permeation characteristics of a lagoon ash. J Test Eval ASTM 28(6):425–430
83. Kolay PK, Singh DN (2001) Physical, chemical, mineralogical and thermal properties of cenospheres from a ash lagoon. Cem Concr Res 31(4):539–542
84. Kolay PK, Singh DN (2001) Effect of zeolitization on physicochemico-mineralogical and geotechnical properties of lagoon ash. Can Geotech J 38(5):1105–1112
85. Kolay PK, Singh DN, Murti MVR (2001) Synthesis of zeolites from a lagoon ash. Fuel 80(5):739–745
86. Kolay PK, Singh DN (2002) Application of coal ash in fluidized thermal beds. J Mater Civ Eng ASCE 14(5):441–444
87. Kolay PK, Singh DN (2002) Characterization of an alkali activated lagoon ash and its application for heavy metal retention. Fuel 81(4):483–489
88. Koshy N, Jha B, Kadali S, Singh DN (2015) Synthesis and characterization of Ca and Na zeolites (non-pozzolanic materials) obtained from fly ash-$Ca(OH)_2$ interaction. Mater Perform Charact ASTM Int 4(1):87–102
89. Koshy N, Singh DN, Jha B, Kadali S, Patil J (2015) Characterization of Na and Ca zeolites synthesized by various hydrothermal treatments of fly ash. Adv Civ Eng Mater ASTM Int 4(1):131–143
90. Koshy N, Singh DN (2016) Fly ash zeolites for water treatment applications. J Environ Chem Eng 4(2):1460–1472
91. Koshy N, Singh DN (2016) Textural alterations in coal fly ash due to alkali activation. J Mater Civ Eng ASCE 28(11):04016126
92. Koshy N, Sushalekshmi SU, Sharma S, Joseph J, Sharma V, Singh DN, Jha B, Singh M (2018) Characterization of the soil samples from the Lonar Crater, India. Geotechn Eng J SEAGS AGSSEA 49(1):99–105
93. Krishnaiah S, Singh DN (2003) Determination of influence of various parameters on thermal properties of soils. Int Commun Heat Mass Transf 30(6):861–870
94. Krishnaiah S, Singh DN (2003) A methodology to determine soil moisture movement due to thermal gradients. J Exp Therm Fluid Sci 27(6):715–721
95. Krishnaiah S, Singh DN (2004) A device for determination of thermal properties of soil. J Test Eval ASTM 32(2):114–119
96. Krishnaiah S, Singh DN (2004) Centrifuge modelling of heat migration in soils. Int J Phys Model Geotech 4(3):39–47
97. Krishnaiah S, Singh DN (2006) Determination of thermal properties of some supplementary cementing material used in cement and concrete. Constr Build Mater 20(3):193–198
98. Krishnaiah S, Singh DN (2006) Determination of thermal properties of soils in a geotechnical centrifuge. J Test Eval ASTM 34(4):319–326
99. Krishnaiah S, Singh DN, Jadhav GN (2004) A methodology for determining thermal properties of rocks. Int J Rock Mech Min Sci 41:877–882
100. Kulkarni MP, Patel A, Singh DN (2010) Application of shear wave velocity for characterizing clays from coastal regions. KSCE J Civ Eng 14(3):307–321
101. Kumar PR, Singh DN (2005) A novel technique for monitoring contaminant transport through soils. Environ Monit Assess 109(1–3):147–160
102. Kumar RP, Singh DN (2012) Geotechnical centrifuge modeling of chloride diffusion through soils. Int J Geomech 12(3):327–332
103. Liu Y (2010) Influence of heating and water-exposure on the liquid limits of GMZ01 and MX80 bentonites. J Rock Mech Geotech Eng 2(2):188–192
104. Mahjoub M, Rouabhi A (2018) Modelling of anisotropic damage due to hydrogen production in radioactive waste disposal. Environ Geotech 5(3):176–183
105. Manthena KC, Singh DN (2001) Centrifuge modeling of soil thermal resistivity. Int J Phys Model Geotech 1(4):29–34
106. Meenu PS, Sowmya S, Latha RA, Shashank BS, Singh DN (2017) Investigations on influence of bio-geo interface on suction characteristics of fine-grained soil. Geotech Geol Eng 35(2):607–614
107. Moayedi H, Asadi A, Moayedi F, Huat BBK (2011) Zeta potential of tropical soil in presence of polyvinyl alcohol. Int J Electrochem Sci 6(5):1294–1306
108. Moghal AAB, Reddy KR, Mohammed SAS, Al-Shamrani MA, Zahid WM (2017) Sorptive response of chromium (Cr^{+6}) and mercury (Hg^{+2}) from aqueous solutions using chemically modified soils. J Test Eval ASTM 45(1):105–119
109. Mondal S, Dangayach S, Singh DN (2018) Establishing heat-transfer mechanisms in dry sands. Int J Geomech ASCE 18(3):06017024
110. Mondal S, Padmakumar GP, Sharma V, Singh DN, Baghini MS (2016) A methodology to determine thermal conductivity of soils from flux measurement. Geomech Geoeng Int J 11(1):73–85
111. Mondal S, Sharma V, Apte P, Singh DN (2018) Electrical analogy for modelling thermal regime and moisture distribution in sandy soils. Geomech Geoeng Int J 13(1):22–32
112. Mondal S, Sharma V, Singh DN, Baghini MS (2018) Detection of thermal response of geomaterials: a critical appraisal. Emerg Mater Res 7(3):1–14
113. Mondal S, Sharma V, Singh DN, Baghini MS (2017) Determination of thermal regime in sandy soils: a mathematical framework ATHERES. Int J Geomech ASCE 17(9):04017045
114. Mualem Y (1976) A new model for predicting hydraulic conductivity of unsaturated porous media. Water Resour Res 12:593–622
115. Palaparthy VS, Baghini MS, Singh DN (2013) Review of polymer-based sensors for agriculture-related applications. Emerg Mater Res 2(4):166–180
116. Palaparthy V, Singh DN, Baghini MS (2017) Compensation of temperature effects for in-situ soil moisture measurement by DPHP sensor. Comput Electron Agric 141:73–80
117. Parlak M (2011) Effect of heating on some physical, chemical and mineralogical aspects of forest soil. J Bartın Orman Fakültesi Dergisi 1(3(19)):143–152
118. Patel A, Bartake PP, Singh DN (2009) An empirical relationship for determining shear wave velocity in granular materials

accounting for grain morphology. Geotech Test J ASTM 32(1):1–10
119. Patel A, Kulkarni MP, Bartake PP, Rao KV, Singh DN (2011) A methodology for determination of resilient modulus of asphaltic concrete. Adv Civ Eng 1:936395
120. Patel A, Singh DN (2009) A generalized relationship for estimating shear wave velocity in soils. Int J Geotech Eng 3(3):343–351
121. Patel A, Singh DN, Singh KK (2010) Performance analysis of piezoceramic elements in soils. Geotech Geol Eng 28:681–694
122. Patel A, Singh KK, Singh DN (2012) Application of piezoceramic elements for determining elastic properties of soils. Geotech Geol Eng 30:407–417
123. Patent No. 277842. A methodology for determination of swelling properties of soils from suction measurements (Indian Patent Application No. 2579/MUM/2012), Granted 2016
124. Patent No. 277862. A novel method for determining cracking characteristics of fine-grained soils using laser microscopy (Indian Patent Application No. 2578/MUM/2012), Granted 2016
125. Patent No. 297124. A methodology to determine influence of initial water content and specimen thickness on the SWCC of fine-grained soils (Indian Patent Application No. 2040/MUM/2013), Granted 2018
126. Pathak P, Singh DN, Apte PR, Pandit GG (2016) Statistical analysis for prediction of distribution coefficient of soil-contaminant system. J Environ Eng 142(1):04015054
127. Pathak P, Singh DN, Pandit GG, Apte PR (2014) Establishing sensitivity of distribution coefficient on various attributes of soil-contaminant system. J Hazard Toxic Radioact Waste ASCE 18(1):64–75
128. Pathak P, Singh DN, Pandit GG, Rakesh RR (2014) Determination of distribution coefficient: a critical review. Int J Environ Waste Manag 14(1):27–64
129. Pathak P, Singh DN, Pandit GG, Rakesh RR (2016) Quantification of geomaterial-contaminant interaction: some guidelines. J Hazard Toxic Radioact Waste Manag ASCE 20(1):04015012
130. Patil BS, Anto A, Singh DN (2017) Simulation of municipal solid waste degradation in aerobic and anaerobic bioreactor. Waste Manag Res 35(3):301–312
131. Patil BS, Singh DN (2015) Study of sustainable engineered bioreactor landfill (SEBL) for small communities. J Solid Waste Technol Manag 14:1–14
132. Penumadu D, Dutta AK, Luo X, Thomas KG (2009) Nano and neutron science applications for geomechanics. KSCE J Civ Eng 13(4):233–242
133. Poulose A, Smitha RN, Singh DN (2000) Centrifuge modelling of moisture migration in silty soils. J Geotech Geoenviron Eng ASCE 126(8):748–752
134. Prakash K, Sridharan A, Sudheendra S (2016) Hygroscopic moisture content: determination and correlations. Environ Geotech 3(5):292–301
135. Rajeev KP, Singh DN (2004) Instrumentation and testing methodology for detecting Cl- contaminants in soils. J Test Eval ASTM 32(2):81–87
136. Rajesh S, Rao HB, Sreedeep S, Arnepalli DN (2015) Environmental geotechnology: an indian perspective. Environ Geotech 2(6):336–348
137. Rakesh RR, Singh DN, Nair RN (2009) A methodology for simulating radionuclide diffusion in unsaturated soils. Geotech Geol Eng 27(1):13–21
138. Rakesh RR, Singh DN, Nair RN (2017) Soil-radionuclide interaction under varied experimental conditions. J Hazard Toxic Radioact Waste ASCE 21(1):D4015005
139. Rao BH, Bhat AM, Singh DN (2007) Application of impedance spectroscopy for modeling flow of AC in soils. Geomech Geoeng Int J 2(3):197–206
140. Rao BH, Dalinaidu A, Singh DN (2007) Accelerated diffusion test on the intact rock mass. J Test Eval ASTM 35(2):111–117
141. Rao HB, Singh DN (2008) Determination of diffusion characteristics of intact rock mass: a critical evaluation. Geotech Test J 31(6):490–502
142. Rao BH, Singh DN (2012) Establishing SWCC and determination of unsaturated hydraulic conductivity of kaolin by ultra centrifugation and electrical measurements. Can Geotech J 49(12):1369–1377
143. Rao BH, Venkataramana K, Singh DN (2011) Studies on determination of swelling properties of soils from suction measurements. Can Geotech J 48(3):375–387
144. Rao SM, Rao PR, Malini R (2014) Environmental geotechnics: need for regional approach. Environ Geotech 1(1):66–67
145. Reddy KR, Adams JA (2001) Effects of soil heterogeneity on air flow patterns and hydrocarbon removal during in-situ air sparging. J Geotech Geoenviron Eng 127(3):234–247
146. Reddy KR, Chinthamreddy S, Saichek RE, Cutright TJ (2003) Nutrient amendment for the bioremediation of a chromium-contaminated soil by electrokinetics. Energy Sources 25(9):931–943
147. Reddy KR, Kulkarni HS, Giri RK, Khire MV (2017) Horizontal trench system effects on leachate recirculation in bioreactor landfills. Geomech Geoeng Int J 12(2):115–136
148. Reddy KR, Kumar G, Giri RK (2017) Influence of dynamic coupled hydro-bio-mechanical processes on response of municipal solid waste and liner system in bioreactor landfills. Waste Manag 63:143–160
149. Reddy NG, Rao BH, Reddy KR (2018) Biopolymer amendment for mitigating dispersive characteristics of red mud waste. Géotech Lett 8(3):1–24
150. Rohini K, Singh DN (2004) A methodology for determination of electrical properties of soils. J Test Eval ASTM 32(1):64–70
151. Rouf MA, Singh RM, Bouazza A, Rowe RK, Gates WP (2016) Gas permeability of partially hydrated geosynthetic clay liner under two stress conditions. Environ Geotech 3(5):325–333
152. Rowe RK (2014) Performance of GCLS in liners for landfill and mining applications. Environ Geotech 1(1):3–21
153. Rowe RK (2015) Reflections on the evolution of geoenvironmental engineering. Environ Geotech 2(2):65–67
154. Sarhosis V, Hosking LJ, Thomas HR (2018) Carbon sequestration potential of the south wales coalfield. Environ Geotech 5(4):234–246
155. Shah PH, Singh DN (2004) A simple methodology for determining electrical conductivity of soils. J ASTM Int 1(5):1–11
156. Shah P, Singh DN (2005) Generalized Archie's law for estimation of soil electrical conductivity. J ASTM Int 2(5):1–20
157. Shah PH, Singh DN (2006) Methodology for determination of hygroscopic moisture content of soils. J ASTM Int 3(2):1–14
158. Shah PH, Sreedeep S, Singh DN (2006) Evaluation of methodologies used for establishing soil-water characteristic curve. J ASTM Int 3(6):1–11
159. Shanthakumar S, Singh DN, Phadke RC (2008) Flue gas conditioning for reducing suspended particulate matter from thermal power stations. Prog Energy Combust Sci 34(6):685–695
160. Shanthakumar S, Singh DN, Phadke RC (2008) Influence of flue gas conditioning on fly ash characteristics. Fuel 87:3216–3222
161. Shanthakumar S, Singh DN, Phadke RC (2009) The effect of dual flue gas conditioning on fly ash characteristics. J Test Eval ASTM 37(6):1–8
162. Shanthakumar S, Singh DN, Phadke RC (2010) Methodology for determining particle-size distribution characteristics of fly ashes. J Mater Civ Eng ASCE 22(5):435–442
163. Shanthakumar S, Singh DN, Phadke RC (2011) Determining residual ammonia in flue gas conditioned fly ashes and its influence on the pozzolanic activity. J Test Eval ASTM 39(1):69–76

164. Sharma S, Singh DN (2015) Characterization of sediments for sustainable development: state of the art. Mar Georesour Geotechnol 33(5):447–465
165. Sharma S, Meenu PS, Asha Latha R, Shashank BS, Singh DN (2016) Characterization of sediments from the sewage disposal lagoons for sustainable development. Adv Civil Eng Mater ASTM Int 5(1):1–23. https://doi.org/10.1520/ACEM20150010
166. Shashank BS, Minto JM, Singh DN, ElMountassir G, Knapp CW (2018) Guidance for investigating calcite precipitation by urea hydrolysis for geomaterials. J Test Eval ASTM 46(4):1527–1538. https://doi.org/10.1520/JTE20170122
167. Shashank BS, Sharma S, Sowmya S, Asha Latha R, Meenu PS, Singh DN (2016) State-of-the-art on geotechnical engineering perspective on bio-mediated processes. Environ Earth Sci 75(3):270. https://doi.org/10.1007/s12665-015-5071-6
168. Shetty R, Singh DN (2018) Rheological characteristics of fine-grained soil-slurries. J Test Eval ASTM 46(6):2351–2363. https://doi.org/10.1520/JTE20170035
169. Shetty R, Singh DN (2017) Utilization of dredged sediments: contemporary issues. J Waterway Port Coastal Ocean Eng ASCE 143(3):04016025
170. Shetty R, Zhang X, Coussot P, Singh DN (2018) "A" Complex Fluid" approach for determining rheological characteristics of the fine-grained soils and clay minerals. J Mater Civ Eng ASCE, in print
171. Shinde SB, Kala VU, Kadali S, Tirumkudulu MS, Singh DN (2012) A novel methodology for measuring the tensile strength of expansive clays. Geomech Geoeng Int J 7(1):15–25
172. Simkovic I, Dlapa P, Doerr SH, Mataix-Solera J, Sasinkova V (2008) Thermal destruction of soil water repellency and associated changes to soil organic matter as observed by FTIR spectroscopy. CATENA 74(3):205–211
173. Singh DN (2014) Editorial. Environ Geotech 1(1):1–2
174. Singh DN, Devid K (2000) Generalized relationships for estimating soil thermal resistivity. Exp Therm Fluid Sci 22:133–143
175. Singh DN, Gangadhara Rao MVBB (1998) Laboratory determination of soil thermal resistivity. Geotech Eng Bull 7(3):179–189
176. Singh DN, Gupta AK (2001) Falling-head conductivity tests in a geotechnical centrifuge. J Test Eval ASTM 29(3):258–263
177. Singh DN, Gupta AK (2000) Modelling hydraulic conductivity in a small centrifuge. Can Geotech J 37(5):1150–1155
178. Singh DN, Kolay PK (2002) Simulation of ash-water interaction and its influence on ash. Prog Energy Combust Sci 28:267–299
179. Singh DN, Kuriyan SJ (2002) Estimation of hydraulic conductivity of unsaturated soils using a geotechnical centrifuge. Can Geotech J 39(3):684–694
180. Singh DN, Kuriyan SJ (2003) Estimation of unsaturated hydraulic conductivity using soil suction measurements obtained by an insertion tensiometer. Can Geotech J 40(2):476–483
181. Singh DN (2016) From nowhere to somewhere. In: Ghosh P, Raj B (eds) The mind of an engineer. Springer, New York, pp 143–147
182. Singh DN, Devid K, Naidu AD (2003) Fabrication of thermal probes for estimation of soil thermal resistivity. J Test Eval ASTM 31(1):65–72
183. Singh DN, Kolay PK, Rao AK (2002) A new approach to study leaching of fly ash from landfills. J Solid Waste Technol Manag 28(3):138–144
184. Singh DN, Kuriyan SJ, Chakravarthy M (2001) A generalized relationship between soil electrical and thermal resistivities. J Exp Therm Fluid Sci 25(3–4):175–181
185. Singh DN, Kuriyan SJ, Madhuri V (2001) Application of a geotechnical centrifuge for estimation of unsaturated soil hydraulic conductivity. J Test Eval ASTM 29(6):556–562
186. Singh KK, Singh DN, Ranjith PG (2016) Effect of sample size on the fluid flow through a single fractured granitoid. J Rock Mech Geotech Eng 8(3):329–340
187. Singh KK, Singh DN, Ranjith PG (2015) Laboratory simulation of flow through single fractured granite. Rock Mech Rock Eng 48(3):987–1000
188. Singh KK, Singh DN, Ranjith PG (2014) Simulating flow through fractures in a rockmass using analog material. Int J Geomech 14(1):8–19
189. SoilVision 4.18. A knowledge-based database system for soil properties. SoilVision Systems Ltd., Saskatoon, Saskatchewan, Canada, 2005
190. Sowmya S, Meenu PS, Asha Latha R, Singh DN (2017) Laboratory investigations on the effects of bacteria on fine-grained soils. Adv Eng Forum 21:352–357
191. Sreedeep S, Singh DN (2011) A critical review of the methodologies employed for soil suction measurement. Int J Geomech ASCE 11(2):99–104
192. Sreedeep S, Singh DN (2008) A novel technique for studying diffusion of contaminants in fine-grained soils. Geomech Geoeng Int J 3(3):199–209
193. Sreedeep S, Singh DN (2005) A study to investigate influence of soil properties on its suction. J Test Eval ASTM 31(1):579–584
194. Sreedeep S, Singh DN (2005) Estimating unsaturated hydraulic conductivity of fine-grained soils using electrical resistivity measurements. J ASTM Int 2(1):1–11
195. Sreedeep S, Singh DN (2006) Methodology for determination of osmotic suction of soils. Geotech Geol Eng 24(5):469–479
196. Sreedeep S, Singh DN (2006) Nonlinear curve-fitting procedures for developing soil-water characteristic curves. Geotech Test J ASTM 29(5):409–418
197. Sreedeep S, Reshma AC, Singh DN (2005) Generalized relationship for determining soil electrical resistivity from its thermal resistivity. Exp Therm Fluid Sci 29:217–226
198. Sreedeep S, Reshma AC, Singh DN (2004) Measuring soil electrical resistivity using a resistivity box and a resistivity probe. Geotech Test J ASTM 27(4):411–415
199. Sultan N, Delage P, Cui YJ (2002) Temperature effects on the volume change behavior of boom clay. Eng Geol 64(2–3):135–145
200. Susha Lekshmi SU, Prathyusha JNV, Aravind P, Singh DN, Bhagini MS (2016) A critical analysis of the performance of plate- and point-electrodes for determination of electrical properties of the soil mass. Measurement 93:552–562
201. Susha Lekshmi SU, Singh DN, Tarantino A, Baghini MS (2018) Evaluation of the performance of TDR and capacitance techniques for soil moisture measurement. Geotech Test J ASTM 41(2):292–306
202. Susha Lekshmi SU, Singh DN, Tarantino A, Baghini MS (2018) Investigations on magnetic characteristics of the soil and their influence on its dielectric response. Appl Clay Sci 158:113–122
203. Susha Lekshmi SU, Singh DN, Baghini MS (2014) A critical review of soil moisture measurement. Measurement 54:92–105
204. Tanaka N, Graham J, Crilly T (1997) Stress–strain behaviour of reconstituted illitic clay at different temperatures. Eng Geol 47(4):339–350
205. Tan Ö, Yilmaz L, Zaimoğlu AS (2004) Variation of some engineering properties of clays with heat treatment. Mater Lett 58(7–8):1176–1179
206. Taguchi G, Konishi S (1987) Taguchi methods, orthogonal arrays and linear graphs: Tools for quality engineering. American Supplier Institute, Dearborn
207. Tej PR, Singh DN (2013) Estimation of tensile strength of soils from penetration resistance. Int J Geomech 13(5):496–501
208. Thakur VKS, Singh DN (2005) Rapid determination of swelling pressure of clay minerals. J Test Eval ASTM 33(4):1–7

209. Thakur VKS, Sreedeep S, Singh DN (2005) Parameters affecting soil water characteristic curves of fine-grained soils. J Geotech Geoenviron Eng ASCE 131(4):521–524
210. Thakur VKS, Sreedeep S, Singh DN (2006) Laboratory investigations on extremely high suction measurements for fine-grained soils. Geotech Geol Eng 24(3):565–578
211. Thakur VKS, Sreedeep S, Singh DN (2007) Evaluation of various pedo-transfer functions for developing soil water characteristic curve for a silty soil. Geotech Test J ASTM 30(1):25–30
212. Uday KV, Singh DN (2013) Application of laser microscopy for studying crack characteristics of fine-grained soils. Geotech Test J ASTM 36(1):146–154
213. Uday KV, Singh DN (2013) Investigations on cracking characteristics of fine-grained soils under varied environmental conditions. Drying Technol 31(11):1255–1266
214. Uday KV, Prathyusha JNV, Singh DN (2014) A generalized relationship for determination of tensile strength of fine-grained soils from shrinkage characteristics. Drying Technol 32:869–876
215. Uday KV, Prathyusha JNV, Singh DN, Apte PR (2015) Application of Taguchi method in establishing criticality of parameters that influence cracking characteristics of fine-grained soils. Drying Technol 33(9):1138–1149
216. Ulery AL, Graham RC (1993) Forest fire effects on soil color and texture. Soil Sci Soc Am J 57(1):135–140
217. Van Genuchten MT (1980) A closed form equation for predicting the hydraulic conductivity of unsaturated soils. Soil Soc Am J 44:892–898
218. Vane LM, Zhang GM (1997) Effects of aqueous phase properties on clay particle zeta potential and electro-osmotic permeability: implications for electro-kinetic soil remediation processes. J Hazard Mater 55(1–3):1–22
219. Venkataramana K, Rao BH, Singh DN (2009) A critical review of the methodologies employed for determination of tensile strength of the fine-grained soils. J Test Eval ASTM 37(2):115–121
220. Wang XS (2011) Batch sorption of lead (II) from aqueous solutions using natural kaolinite. Int J Environ Waste Manag 8(3–4):258–272
221. Welzel U, Ligot J, Lamparter P, Vermeulen AC, Mittemeijer EJ (2005) Stress analysis of polycrystalline thin films and surface regions by X-ray diffraction. J Appl Crystallogr 38(1):1–29
222. West LJ, Stewart DL (1995) Effect of zeta potential on soil electrokinesis. Geoenvironment 2000. ASCE Spec Publ 46:1535–1549
223. Witthüser K, Dalinaidu A, Singh DN (2006) Investigations on diffusion characteristics of granite and chalk rock mass. Geotech Geol Eng 24(2):325–334
224. Wu XF, Zhou G (2011) Application of improved Taguchi method to the multi response optimization. In: I Industrial Engineering and Engineering Management, IEEE 18th international conference on Institute of Electrical and Electronics Engineers, Beijing, China, vol 3, pp 1829–1832
225. Yilmaz G (2011) The effects of temperature on the characteristics of kaolinite and bentonite. Sci Res Essays 6(9):1928–1939
226. Yukselen Y, Kaya A (2003) Zeta potential of kaolinite in the presence of alkali, alkaline earth and hydrolyzable metal ions. J Water Air Soil Pollut 145(1–4):155–168
227. Yun TS, Santamarina JC (2008) Fundamental study of thermal conduction in dry soils. Granul Matter 10(3):197–207
228. Zhang Y, Miao L, Wang F (2011) Study on the engineering properties of the stabilized mucky clay as backfill material in highway embankment projects. Geo-Frontiers 2011: Advances in Geotechnical Engineering, ASCE, 2011, pp 1365–1371

Devendra Narain Singh